공학박사 학위논문

Ergonomics Studies on Working Posture and Movement for Reducing Risk of Work-related Musculoskeletal Disorders

작업 관련 근골격계 질환의 위험성 저감을 위한 작업 자세 및 동작의 인간공학 연구

2022 년 1 월

서울대학교 대학원

산업공학과

정 해 석

Ergonomics Studies on Working Posture and Movement for Reducing Risk of Work-related Musculoskeletal Disorders

근골격계질환의 위험성 저감을 위한 작업 자세 및 동작의 인간공학 연구

지도교수 박 우 진

이 논문을 공학박사 학위논문으로 제출함

2022 년 1 월

서울대학교 대학원

산업공학과

정 해 석

정해석의 공학박사 학위논문을 인준함

2022 년 1 월

위 원 장 윤 명 환 (인)

부위원장 박 우 진 (인)

위 원 이 재 욱 (인)

위 원 황 동 욱 (인)

위 원 백 동 현 (인)

Abstract

Ergonomics Studies on Working Posture and Movement for Reducing Risk of Work-related Musculoskeletal Disorders

Haesuk Jung

Department of Industrial Engineering

The Graduate School

Seoul National University

Working in stressful postures and movements increases the risk of work-related musculoskeletal disorders (WMSDs). The physical stress on a worker's musculoskeletal system depends on the type of work task. In the case of sedentary work, stressful sitting postures for prolonged durations could increase the load on soft connective tissues such as muscles and ligaments, resulting in the incidence of WMSDs. Therefore, to reduce the WMSDs, it is necessary to monitor a worker's sitting posture and additionally provide ergonomic interventions. When the worker performs a task that involves dynamic movements, such as manual lifting, the worker's own body mass affects the physical stress on the musculoskeletal system. In the global prevalence of obesity in the workforce, an increase in the body weight of the workers could adversely affect the musculoskeletal system during the manual lifting task. Therefore, obesity could be

associated with the development of WMSDs, and the impacts of obesity on workers' movement during manual lifting need to be examined.

Despite previous research efforts to prevent WMSDs, there still exist research gaps concerning ergonomics design of work systems. For sedentary workers, a promising solution to reduce the occurrence of WMSDs is the development of a system capable of monitoring and classifying a seated worker's posture in real-time, which could be utilized to provide feedback to the worker to maintain a posture with a low-risk of WMSDs. However, the previous studies in relation to such a posture monitoring system lacked a review of the ergonomics literature to define posture categories for classification, and had some limitations in widespread use and user acceptance. In addition, only a few studies related to obesity impacts on manual lifting focused on severely obese population with a body mass index (BMI) of 40 or higher, and, analyzed lifting motions in terms of multi-joint movement organization or at the level of movement technique.

Therefore, the purpose of this study was to: 1) develop a sensor-embedded posture classification system that is capable of classifying an instantaneous sitting posture as one of the posture categories discussed in the ergonomics literature while not suffering from the limitations of the previous system, and, 2) identify the impacts of severe obesity on joint kinematics and movement technique during manual lifting under various task conditions. To accomplish the research objectives, two major studies

were conducted.

In the study on the posture classification system, a novel smart chair system was developed to monitor and classify a worker's sitting postures in real-time. The smart chair system was a mixed sensor system utilizing six pressure sensors and six infrared reflective distance sensors in combination. For a total of thirty-six participants, data collection was conducted on posture categories determined based on an analysis of the ergonomics literature on sitting postures and sitting-related musculoskeletal problems. The mixed sensor system utilized a kNN algorithm for posture classification, and, was evaluated in posture classification performance in comparison with two benchmark systems that utilized only a single type of sensors. The mixed sensor system yielded significantly superior classification performance than the two benchmark systems.

In the study on the manual lifting task, optical motion capture was conducted to examine differences in joint kinematics and movement technique between severely obese and non-obese groups. A total of thirty-five subjects without a history of WMSDs participated in the experiment. The severely obese and non-obese groups show significant differences in most joint kinematics of the ankle, knee, hip, spine, shoulder, and elbow. There were also significant differences between the groups in the movement technique index, which represents a motion in terms of the relative contribution of an individual joint degree of freedom to the box trajectory in a manual lifting task. Overall,

the severely obese group adopted the back lifting technique (stoop) rather than the leg lifting technique (squat), and showed less joint range of excursions and slow movements compared to the non-obese group.

The findings mentioned above could be utilized to reduce the risk of WMSDs among workers performing various types of tasks, and, thus, improve work productivity and personal health. The mixed sensor system developed in this study was free from the limitations of the previous posture monitoring systems, and, is low-cost utilizing only a small number of sensors; yet, it accomplishes accurate classification of postures relevant to the ergonomic analyses of seated work tasks. The mixed sensor system could be utilized for various applications including the development of a real-time posture feedback system for preventing sitting-related musculoskeletal disorders. The findings provided in the manual lifting study would be useful in understanding the potential risk of WMSDs for severely obese workers. Differences in joint kinematics and movement techniques between severely obese and non-obese groups provide practical implications concerning the ergonomic design of work tasks and workspace layout.

Keywords: Work-related musculoskeletal disorders, Physical load, Posture classification system, Sitting posture, Manual lifting, Obesity, Joint kinematics, Movement technique

Student Number: 2015-21150

Contents

List of Tables

List of Figures

Chapter 1

Introduction

1.1 Research Background

Working in stressful sitting postures has been associated with physical discomfort in the upper body areas [1]–[3] and increased risks of work-related musculoskeletal disorders (WMSD) [4]–[7]. Much research has been conducted to determine and characterize high- and low-risk sitting postures [8]–[17]. Existing studies and recommendations generally portray stressful, high-risk sitting postures as possessing some of the following characteristics: lumbar lordosis with excessive anterior pelvic tilt, sideward bending of the neck or trunk, convex low back, excessive trunk inclination, trunk unsupported by seatback, twisted trunk, and unbalanced postures [8]–[12]. On the other hand, low-risk, recommendable postures were typically described in terms of normal lumbar lordosis with lower back support, normal thoracic kyphosis, and lateral symmetry [8]–[10], [13]–[17].

Working in high-risk sitting postures for prolonged durations must be avoided. However, most individuals find it difficult to avoid adopting high-risk sitting postures because it requires continually monitoring one's own posture and making corrective adjustments upon detecting the occurrence of undesirable postural changes while simultaneously conducting one or more primary cognitive tasks. The postural task and

the primary cognitive tasks would compete for a limited attention capacity [18]–[20]. As the worker directs attention to the primary cognitive tasks at hand, the postural task may become unattended, and, adverse postural changes may occur without the worker's awareness.

A promising solution to the above-mentioned problem is to develop an external posture feedback or warning system, which continually monitors the worker's posture, detects the occurrence of a stressful posture, and, provides a warning through an effective yet non-distracting display. Such a feedback/warning system would help workers easily detect and correct stressful postures with minimal distractions, and, therefore, would help reduce prolonged use of high-risk postures. Creating it, on the other hand, requires developing a sub-system capable of monitoring and classifying a seated worker's postures in real-time.

When the worker performs a task that involves dynamic movements, such as manual lifting, the worker's own body mass could affect the physical stress on the musculoskeletal system. In the global prevalence of obesity in the workforce, an increase in the body weight of the workers could adversely affect the musculoskeletal system during the manual lifting task. In addition, obesity not only increases the weight of the body segments but also reduces the work capacity, as there may be decreased joint range of motion (ROM) and muscle strength per body mass. Therefore, obesity could be associated with the development of WMSDs, and the impacts of obesity on lifting

movement need to be examined.

Obesity is a physical condition defined as abnormal or excessive fat accumulation of the body [21]. The body mass index (BMI), calculated as mass/height^2 (unit: kg/m^2), is an indicator of overall adiposity and is moderately correlated with percent body fat [22], [23]. A person is classified as non-obese if the BMI is less than 25 kg/m^2, overweight if it is greater than or equal to 25 kg/m^2 and less than 30 kg/m^2, and obese if it falls within the range of 30 kg/m^2 or higher. The condition of obesity is further subdivided into different categories: obesity class I (30 kg/m^2 $\leq$ BMI $<$ 35 kg/m^2), obesity class II (35 kg/m^2 $\leq$ BMI $<$ 40 kg/m^2), and obesity class III (40 kg/m^2 $\leq$BMI) corresponding to severe or morbid obesity [24], [25].

Overweight and obesity have increased in the last several decades and are currently prevalent worldwide. From 1975 to 2014, the worldwide prevalence of obesity has increased from 3.2% to 10.9% in men, and from 6.4% to 14.9% in women; if the trends continue, 18% of men and 21% of women are expected to be obese by 2025 [26]. According to the World Health Organization, 1.9 billion adults worldwide were estimated to be overweight in 2016, of which 650 million, or 13% of adults, were obese [21]. Severe obesity also accounts for a nontrivial portion of the global population. For example, in the United States, the prevalence of severe obesity was 7.7% among adults aged 20 years or older in 2015-2016 [27]. The obesity prevalence of the workforce follows that of the general population and obesity rates among various occupational groups

increased significantly over time [28]. In the United States workforce, the obesity rate doubled from about 15% to 30% between 1986 and 2011 [29].

Obesity is associated with decreases in work capacity. The presence of excessive adipose tissue adversely affects the capacity of the neuromusculoskeletal system, including the joint range of motion, muscle strength, power generation, and reaction time [30]–[37]. Work task design that does not take into account the characteristics of obese workers is thought to be part of the causes of work-related musculoskeletal disorders (WMSDs) in the obese workforce. It may also be related to the productivity loss, higher absenteeism, and higher lifetime cost due to disabilities of obese workers [38]–[40].

1.2 Research Objectives

This study developed a sensor-embedded smart chair system that is capable of monitoring and correctly classifying a sitting posture, and investigated the impacts of severe obesity on joint kinematics and movement techniques during manual lifting. The dissertation consisted of two major studies in relation to the research objectives. The objectives of this study were as follows:

- Study 1) Develop a sensor-embedded smart chair system that is capable of monitoring and classifying an instantaneous sitting posture as one of the posture categories discussed in the ergonomics literature while not suffering from the limitations of the previous posture monitoring systems.

- Study 2) Examine the impacts of severe obesity on joint kinematics and movement techniques during manual lifting under various task conditions, and provide a basis for ergonomic interventions or work task design for high BMI individuals.

1.3 Dissertation Outline

This dissertation consisted of two major studies in relation to the research objectives presented in Chapter 1.2. In the study on the posture classification system, a sensor-embedded smart chair system was developed. In the study on the manual lifting task, obesity impacts on joint kinematics and movement technique during manual load lifting were investigated. The overall structure of this dissertation took the form of five chapters (Figure 1.1). Brief descriptions of the chapters were presented below.

In Chapter 1, the research background and objectives were described. The overall structure of the dissertation was also presented.

In Chapter 2, previous studies on sitting-related musculoskeletal disorders and systems for monitoring a seated worker's postures were reviewed. Then, the impacts of obesity on work capacity and biomechanical demands were described.

In Chapter 3, the process of developing the sensor-embedded smart chair system for posture classification was described in detail. The mixed sensor system and two benchmark systems were compared in posture classification performance.

In Chapter 4, the impacts of obesity on manual lifting were investigated. Participant groups were divided into two levels based on the BMI (non-obese and severely obese), and a total of four lifting task conditions were considered in this study. Kinematic variables and movement technique indexes were utilized to characterize the lifting movements.

In Chapter 5, the summary and implications of this study were presented. Then, some limitations were described along with future directions.

Figure 1.1: The overall structure of the dissertation

Chapter 2

Literature Review

2.1 Work-related Musculoskeletal Disorders Among Sedentary Workers

2.1.1 Relationship Between Sitting Postures and Musculoskeletal Disorders

Working in stressful sitting postures has been associated with physical discomfort in the upper body areas [1]–[3] and increased risks of work-related musculoskeletal disorders (WMSD) [4]–[7]. Genaidy et al. [1] reviewed the literature on postural-work activity classification and postural stress analysis in the industry. Liao and Drury [2] demonstrated the relationship between the working posture, discomfort, and performance in a video display terminal (VDT) task. Grandjean and Hünting [3] reviewed standing and sitting postures accompanied by pains in muscle and soft connective tissues of tendons, joints and ligaments. Faucett and Rempel [4] investigated work postures related to the VDT workplace and risk factors for potential musculoskeletal disorders. Head rotation and height of keyboard were significantly related to pain and stiffness in upper body. Ortiz-Hernández et al. [5] analyzed the relationship between WMSDs and use of the computer, and estimated prevalence of

WMSDs among office workers. Healy et al. [7] reviewed practical workplace strategies for reducing prolonged sitting associated with WMSDs, and provided ergonomic interventions at organizational levels.

Much research has been conducted to determine and characterize high- and low-risk sitting postures [8]–[17]. Dul and Hildebrandt [8] discussed the ergonomic guidelines for preventing work-related low back pain. They showed that sitting with a bent posture could be considered a risk factor for low back pain. Some studies [9], [10], [15] discussed standards on working postures and movements concerning the WMSDs, and suggested that excessive motions related to trunk inclination, head inclination, neck flexion/extension, upper arm elevation should be avoided. Vergara and Page [11] measured comfort, postural, and mobility parameters to analyze the cause of trunk discomfort in the sitting posture. Gallagher [12] showed that workers who adopt unusual or restricted postures (e.g., kneeling) are more prone to injury. Kee and Karwowski [13] proposed an assessment technique for postural loading on the upper body. The postural classification scheme of the assessment technique was based on a set of joint motions, including hand, arm, neck, and back, and provided the relative discomfort score for evaluating stress of working posture. Torén [14] quantified the trunk muscle activity according to the angle of axial trunk rotation in sitting posture. The result implies that a twisted trunk could be a risk factor for WMSDs. Tüzün et al. [16] assessed the spine angles of thoracic kyphosis, lumbar lordosis, and sacral inclination with radiological methods, and showed the relationship between the low

back pain and the spine angles. Bodén [17] determined the relationship between passive resistance at trunk rotation and angle of rotation in sitting position. The results show that passive resistance increases progressively with the twisting angle of the trunk, and twisting of the trunk could be a risk factor for low back pain.

Existing studies and recommendations generally portray stressful, high-risk sitting postures as possessing some of the following characteristics: lumbar lordosis with excessive anterior pelvic tilt, sideward bending of the neck or trunk, convex low back, excessive trunk inclination, trunk unsupported by seatback, twisted trunk, and unbalanced postures [8]–[12]. On the other hand, low-risk, recommendable postures were typically described in terms of normal lumbar lordosis with lower back support, normal thoracic kyphosis, and lateral symmetry [8]–[10], [13]–[17].

2.1.2 Systems for Monitoring and Classifying a Seated Worker s Postures

A promising solution to reduce the sitting-related musculoskeletal disorder is to develop an external posture feedback or warning system, which continually monitors the worker's posture, detects the occurrence of a stressful posture, and, provides a warning through an effective yet non-distracting display. Such a feedback/warning system would help workers easily detect and correct stressful postures with minimal distractions, and, therefore, would help reduce prolonged use of high-risk postures. Creating it, on the

other hand, requires developing a sub-system capable of monitoring and classifying a seated worker's postures in real-time.

Multiple research studies have developed systems for monitoring and classifying a seated worker's postures in real-time [41]-[63]. These existing systems may be categorized into three types according to the type of sensors employed: the wearable, image-based, and pressure sensor-embedded systems. The wearable systems typically employed acceleration sensors and/or optical fibers – these sensors were adhered to the skin or were sewn into a garment. These systems classified upper body postures based on the measurement data from the body-worn sensors representing the orientations of the body segments [41]–[43]. Arteaga et al. [41] developed a low-cost wearable system based on the three-axial accelerometer. This system consisted of the accelerometer, beeper, LED light, and vibrator to provide posture warning. Dunne et al. [42] developed and evaluated a system utilizing wearable plastic optical fiber sensors to monitor spinal posture in a sitting position. Nine sensors attached along the spine were used to measure spine flexions and extensions. As a result of comparing spinal posture monitored by the system and expert visual analysis, the system approximated the accuracy in expert visual analysis, and had sufficient reliability. Abyarjoo et al. [43] presented the development and verification of a simple wearable posture monitor system based on the inertial measurement unit. The system also aided in the corrective adjustment of the posture by providing a real-time warning when the user takes a posture with a large deviation from predefined postures.

The image-based systems analyzed video images of a seated worker to classify instantaneous sitting postures [44]–[46]. One or multiple cameras were placed to capture the sagittal and/or frontal plane images of the seated worker. Through the use of a commercial depth camera, Lee et al. [44] proposed a system to prevent forward head posture associated with WMSDs, including chronic neck pain. The system was evaluated in terms of performance and user preference according to the modality utilized in the warning. As the results, very high accuracy was achieved in detecting forward head postures, and the haptic warning showed superior results in the subjective evaluation. Nayak et al. [45] developed a system for providing workers with feedback about their head movements using two cameras. The camera tracked the worker's face, and calculated the distance between the face and the computer screen. The other side-camera monitored the worker's neck posture to calculate the neck orientation described in Euler angles. The system aggregated posture information and working time, and provided graphical feedback when a worker is in a bad posture or needs a break. Manzi et al. [46] presented an activity recognition system based on the joint detection algorithm utilizing depth camera. A support vector machine was employed for activity classification. The developed system was evaluated on two public datasets including various activities as well as sitting posture. The system outperformed state-of-the-art classification methods in terms of precision and recall.

The pressure sensor-embedded systems typically utilized a large array of pressure sensors or a pressure mat placed inside the seat cushion of an office chair to

classify a worker's sitting postures. Many of the recent sitting posture monitoring and classifying systems belonged to this category [47]–[63]. The pressure sensor-embedded systems have been referred to as "smart chairs." They typically employed machine-learning models, such as k-Nearest Neighbor (kNN), neural network, Naïve Bayes, and support vector machine classifiers, for real-time posture classification [47]–[49], [62], [63]. The previous smart chair systems were summarized in Table 2.1.

Mota and Picard [47] presented a system for classifying sitting postures utilizing two matrices of pressure sensors located on the seat pan and seat back of a chair. The system employed a neural network to classify nine sitting postures. The classifier achieved an overall accuracy of 87.6% for postures coming from new subjects. Meyer et al. [48] developed a pressure measurement system adopting textile sensor arrays on the seat pan and seat back. The textile sensor with 240 elements was used for sitting posture classification. A Naive Bayes classifier was used to classify sixteen sitting postures, and showed an accuracy rate of 84%. Ma et al. [49] proposed a posture monitoring system to classify sitting postures in the wheelchair. The system consisted of a total of twelve pressure sensors, and classified five types of sitting postures. The classification models were trained using five supervised classification techniques; decision tree, support vector machines, multilayer perceptron, Naïve Bayes, and k-nearest neighbors. As a result of comparing the models, the decision tree had the highest accuracy of about 99%. Mutlu et al. [50] presented the performance of the posture classification system according to the number of pressure sensors utilized in

the seat back and seat pan. In the case of utilizing thirty-one sensors, the classification accuracy was 87%. Using a near-optimal sensor placement strategy, the system achieved an accuracy of 78% with nineteen sensors while reducing cost and computational complexity. Kamiya et al. [51] classified nine posture categories by attaching sixty-four pressure sensors to the seat pan. Support vector machine was adopted as a classifier, and showed classification rates of 98.9% when the subject was known and 93.9% when the subject was unknown. An intelligent chair that uses pressure sensors to detect and correct posture was developed by Martins et al. [52]. The authors defined eleven posture categories, and achieved a posture classification accuracy of about 80% using neural networks. Xu et al. [53] presented a textile-based sensing system that monitors the sitting posture being accurately and non-invasively. The system was developed by embedding the pressure sensor array in the seat pan. Seven postures were utilized for classification. The recognition rate of the system was in excess of 85.9%. A prototype sensing system was developed by Fu [54] using eight force sensing resistors to detect sitting postures. The sitting posture was defined by dividing it into a leg posture and a spine posture, and classified through a support vector machine. The posture classification performance for unknown subjects was 80.7% for spine posture and 42.3% for leg posture. Scena and Steindler [55] developed a system for characterizing sitting posture by measuring the axial rotation of the trunk and pelvic movement. The axial rotation of trunk and pelvis movement were measured using a potentiometer and pressure distribution of the seat pan, respectively. Shirehjini et al. [56] designed a

system that classifies six postures utilizing decision rules. Each seat back and seat pan was equipped with four pressure sensors. Suzuki et al. [57] measured a time series of the pressure distributions from 16 x 16 pressure sensors on a chair. In this study, various sitting postures were quantified by the distance from the pressure values of neutral posture. Liang et al. [58] developed a low-cost and non-intrusive posture classification system. Fifteen posture categories were considered in this study. An Ensemble method combining a number of different classifiers was adopted for classification. As a result of the classification performance, with more than ten pressure sensors, the precision and recall were at least 85% and 86%, respectively. Zhou and Lukowicz [59] presented a sensing system in the form of a wireless blanket covering seat pan and seat back. Pressure sensors had 1024 sensitive points. Classification was performed on twelve postures, and the accuracy was about 80%. Kim et al. [60] developed a system for real-time sitting posture detection based on washable and highly durable textile pressure sensors. In this study, seven types of sitting postures were successfully classified based on the pressure measurements under the hip, thigh, and back. Roh et al. [61] proposed a system that measures a total of six sitting postures. Four pressure sensors were mounted on the seat pan, and support vector machines using radial basis function kernels achieved a classification rate of 97%. Huang et al. [62] developed a system that utilized pressure sensor arrays to monitor the sitting postures accurately with the neural network classifier. The experimental results showed that the system could classify eight sitting with accuracy of 92%. Zemp et al. [63] developed an chair system

with force and acceleration sensors to identify the user's sitting position by applying five machine learning techniques. A total of sixteen force sensor values and the backrest angle were utilized for classification. The best performance was achieved using the random forest algorithm with classification accuracy of 90.9%.

Table 2.1: Summary of previous smart chair systems

Author	Sensor type	Posture category	Posture classifier	Classification accuracy (%)
Mota and Picard [47]	42 by 48 array of pressure sensors	Leaning forward, leaning forward left, leaning forward right, sitting upright, leaning back, leaning back left, leaning back right, sitting on the edge of seat, slumping back	Neural networks	87.6
Meyer et al. [48]	Textile sensor with 240 elements	Seated upright, leaning right, leaning left, leaning forward, leaning back, left leg crossed over the right, right leg crossed over the left, once seated upright and once leaning back, once while the knees are touching and once with the ankle rested on the leg, slouching, sitting on the leading edge, slouched down	Naïve Bayes	84
Ma et al. [49]	12 force sensitive resistor pressure sensors	Proper sitting, lean left, lean right, lean forward, lean backward	J48 decision tree, Support vector machine, multilayer perceptron, Naïve Bayes, k-Nearest Neighbors	99.48 (J48)

Table 2.1: (Continued)

Author	Sensor type	Posture category	Posture classifier	Classification accuracy (%)
Mutlu et al. [50]	31 force sensing resistors	Left leg crossed, right leg crossed, leaning back, leaning forward, leaning left, leaning right, left leg crossed and leaning right, right leg crossed and leaning left, seated upright, slouching	Logistic regression	87
Kamiya et al. [51]	64 pressure sensors	Normal, leaning forward, leaning backward, leaning right, leaning left, right leg crossed, leaning right with right leg crossed, left leg crossed, leaning left with left leg crossed	Support vector machine	93.9
Martins et al. [52]	8 pressure sensors	Seated upright, leaning forward, leaning back, leaning back with no lumbar support, leaning left, leaning right, right leg crossed, left leg crossed	Neural networks	93.4
Xu et al. [53]	Textile sensor array	Sit up, forward, backward, left lean, right lean, right foot over left, left foot over right	Naïve Bayes	85.9

Table 2.1: (continued)

Author	Sensor type	Posture category	Posture classifier	Classification accuracy (%)
Liang et al. [58]	40 pressure sensors	Sitting upright, slouching, leaning back, leaning forward (angle<30 degrees), leaning forward (angle>45 degrees), leaning left (angle<10 degrees), leaning left (angle>20 degrees), leaning right (angle<10 degrees), leaning right (angle>20 degrees), left leg crossed in ankle, left leg crossed in knee, right leg crossed in ankle, right leg crossed in knee, left leg crossed, leaning right, right leg crossed, leaning left.	Naïve Bayes, SVM, ensemble method (AdaBoost)	85 (AdaBoost)
Zhou and Lukowicz [59]	Pressure mat with 32 by 32 sensing points	Sit straight up, sit with flexed spine and look forward, sit with flexed spine and look deep downward, lean back, lie on chair, reach to left, lean left, slight lean left, reach to right, lean right, slight lean right, not a posture	Simple algorithm proposed by the authors	72.1

Table 2.1: (continued)

Author	Sensor type	Posture category	Posture classifier	Classification accuracy (%)
Kim et al. [60]	Textile pressure sensors with 10 sensing points	Standing, right leg over the left leg, left leg over the right leg, upright sitting, sitting with both legs lifted, back to standing position, leaning back to the left, leaning back to the right, slouching	Decision algorithm	-
Roh et al. [61]	4 load cells	upright sitting with backrest, upright sitting without backrest, front sitting with backrest, front sitting without backrest, left sitting, right sitting	Support vector machine, linear discriminant analysis, quadratic discriminant analysis, Naïve Bayes, random forest, decision tree	97.2 (SVM)
Huang et al. [62]	8 by 8 piezo-resistive sensor array	Upright sitting, slumped sitting, leaning forward, leaning backward, leaning left, leaning right, right leg crossed, left leg crossed	Artificial neural network	92.2

Table 2.1: (continued)

Author	Sensor type	Posture category	Posture classifier	Classification accuracy (%)
Zemp et al. [63]	16 force sensors and accelerometer	upright position, reclined position, forward inclined position, laterally tilted right position, laterally tilted left position, left leg over the right one, right leg over the left one	Support vector machines, multinomial regression, boosting, neural networks, random forest	90.9 (random forest)

2.2 Impacts of Obesity on Manual Works

2.2.1 Impacts of Obesity on Work Capacity

Obesity is associated with decreases in work capacity. The presence of excessive adipose tissue adversely affects the capacity of the neuromusculoskeletal system, including the joint range of motion, muscle strength, power generation, and reaction time [30]–[37]. Work task design that does not take into account the characteristics of obese workers is thought to be part of the causes of work-related musculoskeletal disorders (WMSDs) in the obese workforce. It may also be related to productivity loss, higher absenteeism, and higher lifetime cost due to disabilities of obese workers [38]–[40].

Capodaglio et al. [30] reviewed the physiological and biomechanical causes of reduced work capacity in obese people. In their study, the authors noted that a reduction in work capacity could be attributed to limited or impaired function of the following factors: spine flexibility, endurance, range of movement, muscle strength, posture holding capacity, respiratory capacity, and visual control. Park et al. [31] investigated the effects of obesity on active joint range of motion (ROM). In the measured ROM data, obese people had significantly smaller ROM in the following nine motions: shoulder extensions and adductions, lumbar spine extension and lateral flexions and knee flexions. The decrease in ROM was attributed to mechanical interference and obstruction of joint motion caused by fat accumulation in obese people.

Jeong et al. [32] examined the impacts of pre-obesity and obesity on passive joint ROM. In this study, twenty-two joint ROMs were analyzed based on obesity level by utilizing a publicly available passive ROM dataset. The pre-obese and obese groups showed significantly smaller ROMs in six motions (elbow flexion and supination, hip extension and flexion, knee flexion and ankle plantar flexion) compared to the non-obese group, but there was no significant difference except for knee flexion between the pre-obese and obese groups. Gilleard and Smith [33] identified the effects of obesity on trunk forward flexion in sitting and standing, and hip joint moment during the standing task. The results showed that forward flexion motion of the thoracic segment and thoracolumbar spine was decreased for obese people, and no significant difference was found in the pelvic segment and hip joint motion. As a result, the hip joint moment calculated through these results was significantly greater in obese people, which may provide an explanation for the increased the risk of WMSDs in obese people. Maffiuletti et al. [34] compared the quadriceps femoris muscle strength and fatigue between obese and non-obese groups. Muscle fatigue was quantified by voluntary torque loss during the protocol, and the voluntary torque loss of the obese group was significantly higher than that of the non-obese group. Also, the relative muscle strength normalized with a body mass of the obese group was lower than that of the non-obese group, despite higher absolute muscle strength than the non-obese group. Lafortuna et al. [35] evaluated the difference in muscle strength and power output between the obese and non-obese groups. The maximum muscle strength of the upper and lower limbs was

evaluated by an isotonic machine, and the power output of the lower limbs was measured by a jumping test. The maximum isotonic strength was higher in the obese group than in the non-obese group, but the power generation was similar between the two groups. The findings indicate that the excess fat mass of obese individuals could impair the power generation during jumping. Miyatake et al. [36] examined the differences in leg and grip strength according to age and gender. For both sexes under 60 years of age, grip and leg strength were significantly higher in the obese group than in the non-obese group. On the other hand, the weight-bearing index obtained by dividing leg strength by body weight was significantly lower in the obese group than in the non-obese group. Baek et al. [37] investigated the impacts of obesity on task performance and perceived discomfort during seated foot target reaches. Compared to the non-obese group, the obese group showed longer movement time, reaction time, and performance time. The findings implied that excess fat mass in an obese body could adversely affect physiological and cognitive aspects. The functional impairments associated with obesity in the aforementioned studies may have contributed to the reduction of work capacity in obese individuals.

2.2.2 Impacts of Obesity on Joint Kinematics and Biomechanical Demands

To alleviate the occupational musculoskeletal problems of obese workers and to improve

productivity in the workforce, research has been conducted on the impacts of obesity on physical load and task performance in a variety of physical works. Previous studies examined how obesity affects biomechanical loads in manual lifting [64] and carrying [65], movement kinematics in manual lifting [66]–[69], perceived postural stress in static posture holding [70], functional limitation in reaching [71]–[73], postural stability in manual lifting [74], [75] and quiet standing [76], tolerance limit in manual lifting [70], [77], reaction time in seated foot reaching [37]. These studies provided implications of their findings concerning the ergonomic work task design for obese workers.

Among the above-mentioned studies, several studies examined the impacts of obesity on the joint kinematics, biomechanical loadings, and psychophysical tolerance limits during manual load lifting [64], [66]–[70]. Manual lifting is one of the important risk factors for low back disorders [78]–[80]. Singh et al. [64] and Corbeil et al. [66] predicted the stresses at L5/S1 disc during manual load lifting by utilizing a biomechanical model and found that obese individuals had greater lumbar loading, and, thus, they could be more vulnerable to lifting-related musculoskeletal disorders (MSDs) than non-obese individuals. Colim et al. [69] examined trunk flexion, knee flexion, and pelvis inclination in the presence of a barrier that replicates the industrial bin, and the results demonstrated that the obese subjects had greater trunk acceleration and larger horizontal distance between the ankle and the knuckle, suggesting that they were exposed to a higher risk of MSDs. According to Xu et al. [67], high BMI subjects had significantly higher peak trunk acceleration and velocity when performing free dynamic

lifting. The author's hypothesis that obese people might lift slowly to minimize loading caused by greater body mass and acceleration was not supported by the results. Sangachin and Cavuoto [68] compared the trunk kinematics, heart rate, and task duration of obese and non-obese groups when performing prolonged repetitive lifting. When fatigue occurred due to prolonged lifting, trunk acceleration increased in the obese group over time, which was explained by a change in lifting technique caused by obesity-related characteristics. Singh [70] investigated the psychophysical effects of obesity on lifting tolerance limit and there was no significant difference in the maximum acceptable weights of lift according to the worker's obesity level.

Chapter 3

Developing and Evaluating a Mixed Sensor Smart Chair System for Real-time Posture Classification: Combining Pressure and Distance Sensors

3.1 Introduction

Working in stressful sitting postures has been associated with physical discomfort in the upper body areas [1]–[3] and increased risks of work-related musculoskeletal disorders (WMSD) [4]–[7]. Much research has been conducted to determine and characterize high- and low-risk sitting postures [8]–[17]. Existing studies and recommendations generally portray stressful, high-risk sitting postures as possessing some of the following characteristics: lumbar lordosis with excessive anterior pelvic tilt, sideward bending of the neck or trunk, convex low back, excessive trunk inclination, trunk unsupported by seatback, twisted trunk, and unbalanced postures [8]–[12]. On the other hand, low-risk, recommendable postures were typically described in terms of normal lumbar lordosis with lower back support, normal thoracic kyphosis, and lateral symmetry [8]–[10], [13]–[17].

Working in high-risk sitting postures for prolonged durations must be avoided. However, most individuals find it difficult to avoid adopting high-risk sitting postures

because it requires continually monitoring one's own posture and making corrective adjustments upon detecting the occurrence of undesirable postural changes while simultaneously conducting one or more primary cognitive tasks. The postural task and the primary cognitive tasks would compete for a limited attention capacity [18]–[20]. As the worker directs attention to the primary cognitive tasks at hand, the postural task may become unattended, and, adverse postural changes may occur without the worker's awareness.

A promising solution to the above-mentioned problem is to develop an external posture feedback or warning system, which continually monitors the worker's posture, detects the occurrence of a stressful posture, and, provides a warning through an effective yet non-distracting display. Such a feedback/warning system would help workers easily detect and correct stressful postures with minimal distractions, and, therefore, would help reduce prolonged use of high-risk postures. Creating it, on the other hand, requires developing a sub-system capable of monitoring and classifying a seated worker's postures in real time.

Multiple research studies have developed systems for monitoring and classifying a seated worker's postures in real time. These existing systems may be categorized into three types according to the type of sensors employed: the wearable, image-based, and pressure sensor-embedded systems [41]-[63].

The wearable systems typically employed acceleration sensors and/or optical

fibers – these sensors were adhered to the skin or were sewn into a garment. These systems classified upper body postures based on the measurement data from the body-worn sensors representing the orientations of the body segments [41]–[43]. The image-based systems analysed video images of a seated worker to classify instantaneous sitting postures [44]–[46]. One or multiple cameras were placed to capture the sagittal and/or frontal plane images of the seated worker. Some of these image-based systems were designed to classify the worker's head postures [44], [45].

The pressure sensor-embedded systems typically utilized a large array of pressure sensors or a pressure mat placed inside the seat cushion of an office chair to classify a worker's sitting postures. Many of the recent sitting posture monitoring and classifying systems belonged to this category [47]–[63]. The pressure sensor-embedded systems have been referred to as "smart chairs." They typically employed machine-learning models, such as k-Nearest Neighbor (kNN), neural network, Naïve Bayes, and support vector machine classifiers, for real-time posture classification [47]–[49], [62], [63].

Each of the existing systems mentioned above has been reported to successfully classify seated working postures within its own set of pre-defined posture categories. These systems, however, have some limitations. The wearable systems require the users to wear them, and, thus, are perceived as invasive and inconvenient. The invasiveness and inconvenience can make it difficult for the system to gain a wide user acceptance.

The image-based systems could not serve their purpose when the worker is out of the camera view or obstacles occlude the worker's body parts. In addition, the image-based systems require the user to be exposed to the cameras at all times; this could cause psychological discomfort, which can hinder user acceptance.

The pressure sensor-embedded systems are free from the invasiveness and inconvenience of wearable systems, and the occlusion and psychological discomfort problems of image-based systems. However, these systems relying solely on pressure sensors seem to have some limitations in the posture classification capability – for example, none of the existing systems has been shown to be capable of accurately recognizing trunk rotation, which is important for the ergonomics evaluation of sitting postures. Also, many of these systems require integrating a pressure mat or utilizing a large number of pressure sensors, which makes them rather expensive for wide-spread use.

The long-term goal of our research is to develop an effective real-time posture feedback system that contributes to reducing sitting-related discomfort and musculoskeletal problems. As an initial effort towards this goal, the purpose of the current study was to: 1) develop a novel, affordable, sensor-embedded smart chair system that is capable of monitoring and correctly classifying an instantaneous sitting posture as one of the major sitting posture categories discussed in the ergonomics literature while not suffering from the limitations of the previous posture monitoring

and classification systems, and, 2) empirically validate its posture classification performance. Eleven posture categories relevant to the ergonomics analyses of seated work tasks were identified through an analysis of the ergonomics literature on sitting postures and sitting-related musculoskeletal problems. They included both high- and low-risk sitting postures.

To accomplish the research objectives of the current study, this study adopted a new design strategy of utilizing a small set of infrared reflective distance sensors in combination with a small number of pressure sensors – the distance and pressure sensors were embedded in the seatback and cushion areas, respectively. Thus, the resulting smart chair system was termed the mixed sensor system. The mixed sensor system utilized a kNN algorithm for posture classification - for a given set of sensor measurements, it classified the corresponding posture as one of the predefined posture categories on the basis of a training dataset.

The mixed sensor system was empirically evaluated in posture classification performance in comparison with matching smart chair systems that utilized only a single type of sensors - a pressure sensors only system and a distance sensors only system. The two benchmark systems were identical to the mixed sensor system except that each of them utilized only a single type of sensors; also, they employed a kNN classifier. The comparative evaluation was intended to confirm the utility of the unique design feature of the mixed sensor system, that is, combining seatback distance sensors

and seat cushion pressure sensors, in terms of posture classification performance. In particular, the comparative evaluation was focused on examining if the two sensor clusters (the 6 pressure sensors and the 6 distance sensors) both contribute significantly to the overall performance of the mixed sensor system. 10-fold cross-validation was conducted for the comparative evaluation.

The rest of this article is organized as follows. Section 3.2 describes the design of the mixed sensor system, and, the methods for the comparative evaluation. Section 3.3 describes the results of the posture classification performance evaluation. Finally, Section 3.4 provides a discussion of the study findings.

3.2 Materials and Methods

This section describes the design and development of the mixed sensor system, and, the methods for evaluating its posture classification performance.

3.2.1 Predefined Posture Categories for the Mixed Sensor System

The mixed sensor system was intended to classify an instantaneous sitting posture as one of the predefined posture categories relevant to the ergonomics evaluation of seated work tasks. A total of eleven posture categories were considered in this study (Figure 3.1). They were identified through a review of the existing ergonomics literature on sitting postures and sitting-related musculoskeletal problems, including low back pain, shoulder and back disorders [8]–[17].

The eleven posture categories (Figure 3.1) included both high- and low-risk postures. Posture categories 1 and 2 are considered low in the level of bodily stresses and have been recommended for office workers [10], [13] The other posture categories have been associated with increased risks of WMSD. Forward trunk flexion characterizing posture category 3 has been shown to increase the compression forces on the intervertebral discs [81]. Increased loads on the intervertebral discs have been related to low back pain [82].

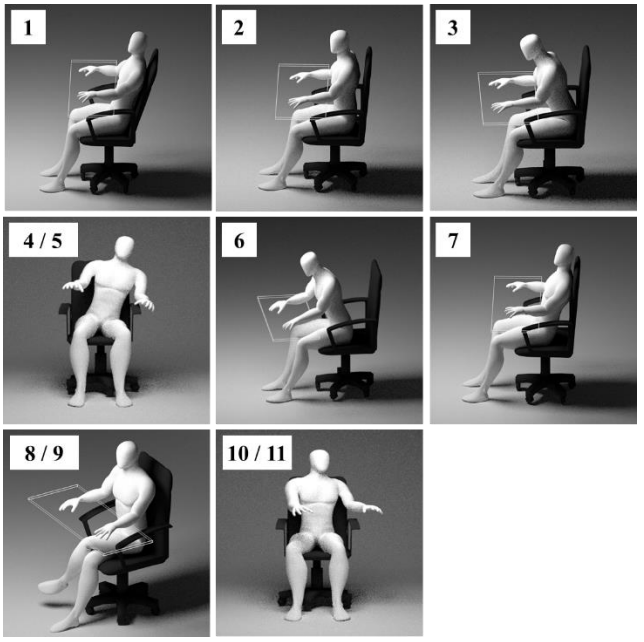

Figure 3.1: Eleven sitting posture categories: (1) Leaning on the seatback while keeping the back straight, (2) detaching the back from the seatback and keeping the trunk erect, (3) flexing the trunk forward about 45 degrees (slouch), (4) leaning against an armrest with lateral bending (left), (5) leaning against an armrest with lateral bending (right), (6) sitting on the leading edge with convex trunk, (7) leaning back with hips slightly forward (slump), (8) legs crossed (left), (9) legs crossed (right), (10) rotating the trunk about 20 degrees (left), and (11) rotating the trunk about 20 degrees (right)

Trunk lateral bending depicted in posture categories 4 and 5 generates asymmetrical compressive loadings on the intervertebral discs. During trunk lateral

bending, the trunk is maintained by imbalanced activities of the erector spinae muscles of the ipsilateral and contralateral sides [83]. Trunk lateral bending during sitting increased antagonistic contractions in the trunk muscle activity and resulted in increased stress concentration in the intervertebral discs [84]. Repetitive lateral bending and unequal stress concentration in the intervertebral discs have been associated with increased risks of low back pain [85].

Posture categories 6 and 7 are characterized by the lack of lumbar support use. The use of a lumbar support reduces the loads exerted on the ischial tuberosities; such off-loading was found to be beneficial to individuals with low back pain [86]. The lack of lumbar support, on the other hand, is known to flatten the lumbar spine, cause tension on the ligaments and other connective tissues in the spine area, and, lead to excessive loads on the discs [87].

The "legs crossed" postures (posture categories 8 and 9) are known to create asymmetric high-pressure regions and increase peak pressures in the hips and thighs, resulting in pain and discomfort [88]. Also, unbalanced gluteal pressure distributions could cause trunk forward leaning during prolonged sitting [89].

Posture categories 10 and 11 involve trunk rotation. Prolonged twist of trunk increases passive resistance that needs to be overcome [17] and has been associated with increased risks of low back pain and WMSDs [14], [90]. The existing smart chair studies did not consider identifying trunk rotation despite its relevance to the

ergonomics evaluation of seated work activities [41]-[63].

3.2.2 Physical Construction of the Mixed Sensor System

The proposed mixed sensor system utilized sensor measurements of seat cushion pressure distribution and seatback-trunk distances to classify sitting postures. A typical height-adjustable office chair with armrests and a headrest was adopted to develop the system (Figure 3.2(a)).

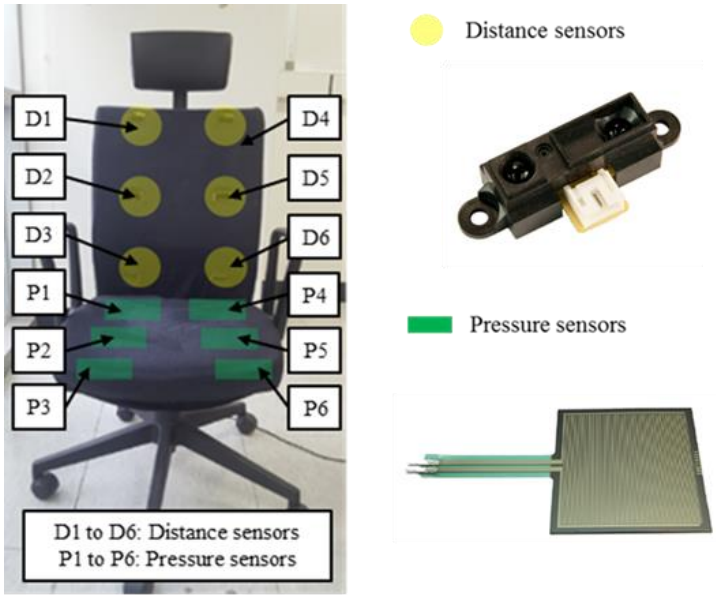

Figure 3.2: Physical construction of the mixed sensor system: (a) placement of sensors, and (b) distance and pressure sensors.

The seat cushion and seatback were equipped with six force sensing resistors (FSRs; “P1” to “P6”) and six infrared reflective sensors (“D1” to “D6”), respectively (Figure 3.2(b)). Each batch of six sensors was arranged in two columns of three. The FSRs embedded beneath the seat cushion surface were to gather the seat cushion pressure distribution data. Each FSR measured the pressure applied to an active surface of a 3.8 cm × 3.8 cm square. One FSR could stably measure up to 10 kgf. The infrared reflective sensors were embedded into small pits created in the seatback cushion in advance. They were to determine the horizontal distances between the seatback and the trunk at different heights for both the left and right sides of the back; therefore, they reflected the upper body posture of the seated worker. The infrared reflective sensors provided stable measurements from 2 cm to 50 cm.

The infrared reflective sensors in the seatback represented a novel design feature, which was not considered in the previous smart chair studies [41]-[63].

The locations of the FSRs and the infrared reflective sensors were determined to ensure that all of the twelve sensors produce valid measurements for at least 99 percent of the Korean adult population – to do so, the anthropometric dataset of the SizeKorea survey was utilized [91]. That is, when a participant with a body size of more than 1 percentile sits in the center of the chair, all pressure sensors could measure valid data by contacting the participant's thigh and seat pan, and the distance sensors could provide the distances between the participant's upper back and the seat back.

The SizeKorea survey was conducted on the basis of ISO 7250 (1996) and ISO 8559 (1989), and the survey participants consisted of 2,196 males and 2,293 females aged between 20 and 69 years. The anthropometric dimensions considered for the determination of the sensor locations were: shoulder height, chest breath, and hip breadth in sitting position (Figure 3.3).

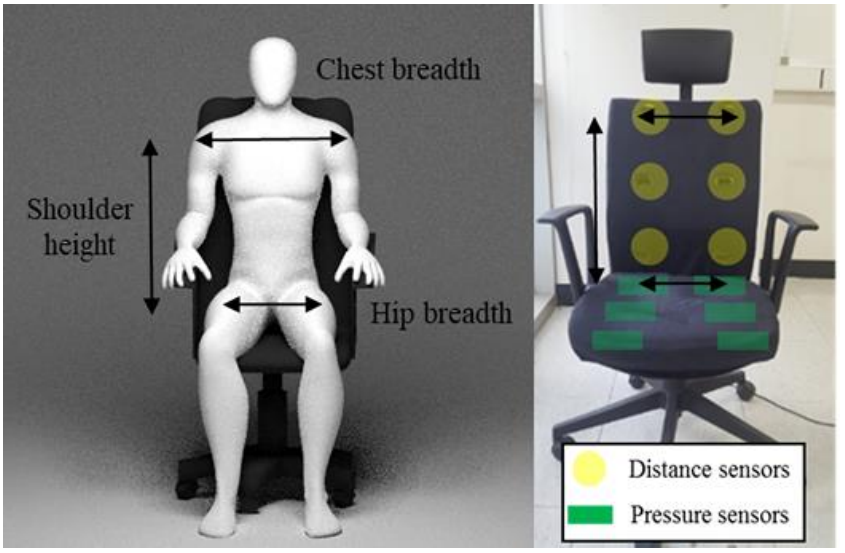

Figure 3.3: Anthropometric dimensions considered for the sensor placement

3.2.3 Posture Classifier Design for the Mixed Sensor System

The mixed sensor system employed a kNN classifier for posture classification. It classifies an instantaneous sitting posture as one of the eleven posture categories in

Figure 3.1, on the basis of the corresponding sensor measurements.

The kNN algorithm is simple and intuitive, and is widely used for various engineering applications that require pattern classification [92]–[94]. A kNN classifier stores a set of training set (training cases and their classes). Each case is a vector in a feature space.

A test case (a new observation to be classified) is classified based on the classes of the k most similar cases (the k nearest neighbors) found in the training dataset - the class of the test case is determined by a majority vote among the classes of the k nearest neighbors.

A weighted Euclidean distance shown in Equation 3.1 was used as the distance function for the kNN classifier; it represents how close the i-th training case x_i is to the test case x_t. In Equation 3.1, x_i represents the normalized N-dimensional feature vector of the i-th training case, and $x_{i,j}$ denotes its j-th element. Similarly, x_t and $x_{t,j}$ denote the normalized feature vector of the test case and its j-th feature value, respectively. The feature vectors were normalized by min-max normalization. w_j is the weight assigned to the j-th feature. The weight w_j reflects the relative importance of the j-th feature [95], [96].

$$d(\mathbf{x_i}, \mathbf{x_t}) = \sqrt{\sum_{j=1}^{N} w_j (x_{i,j} - x_{t,j})^2} \quad with \quad \sum_{j=1}^{N} w_j = 1 \tag{3.1}$$

The feature vector elements, that is, the features, were selected from a set of candidate features. The candidate features included the normalized pressure and/or distance sensor measurements and the pairwise differences of the normalized sensor measurements within each sensor type. The normalized pressure sensor measurements were obtained by dividing each of the original pressure sensor measurements by their sum. The candidate features utilized in the classifier is shown in Table 3.1 – the features are grouped into laterally symmetric pairs.

Table 3.1: List of candidate features

	Candidate features
Pressure-related	P1 & P4, P2 & P5, P3 & P6, P1-P3 & P4-P6, P1-P2 & P4-P5, P2-P3 & P5-P6, P1-P4, P2-P5, P3-P6
Distance-related	D1 & D4, D2 & D5, D3 & D6, D1-D3 & D4-D6, D1-D2 & D4-D5, D2-D3 & D5-D6, D1-D4, D2-D5, D3-D6
Pressure- and distance-related	(D1-D3)*(P3-P1) & (D4-D6)*(P6-P4), (D4-D1)*(P1-P4)

Feature selection was performed utilizing the domain knowledge-guided forward selection method [97]. The feature weights, w_j, in Equation 3.1 were optimized using the grid search method [98], [99] - the model parameters, the feature weights and the number of nearest neighbors, were determined to maximize the match between the class of each case in the training dataset and the class determined through majority voting of k nearest neighbors excluding itself. The weights of the laterally symmetric features were constrained to be identical. The hyperparameter k was determined within the range from 2 to 15. Each weight w_j was determined within the grid range from 0 to 2 with the increment of 0.02, and, was divided by the total sum of the weight.

3.2.4 Data Collection for Training and Testing the Posture Classifier of the Mixed Sensor System

Data collection was conducted to gather labeled sensor measurement data for training and testing the kNN classifier of the mixed sensor system. A total of thirty-six individuals participated in the data collection. The demographic information of the participants is summarized in Table 3.2. The participants performed a single posture measurement trial for each of the eleven posture categories shown in Figure 3.1. In each trial, the participants were asked to maintain the corresponding posture for 10 seconds while sitting on the chair of the mixed sensor system. The order of the eleven posture categories was randomized for each participant. In order to help the participants

correctly adopt and maintain the postures shown in Figure 3.1, the experimenters utilized external visual references (markings on the side wall and the desktop) depicting the trunk forward flexion angle (45 degrees) for posture category 3 and the trunk rotation angle (20 degrees) for posture categories 10 and 11. For the rest of the posture categories, the participants and the experimenters relied on the visual images shown in Figure 3.1 and the associated verbal descriptions.

Detailed instructions for each posture category were as follows. All posture categories were based on positioning the hip close to the seat back, placing both hands on the desk, and facing the front (base posture). For the posture category 1, participants were instructed to lean the trunk on the seat back with the base posture. For the posture categories 2 and 3, the participants were additionally guided to erect the trunk or tilt it forward about 45 degrees. For the posture categories 4 and 5, participants tilted their upper body to the left or right by about 30 degrees. For the posture category 6, the hip was moved to the midpoint of the seat pan so that lumbar support was not used. For the posture category 7, the upper back was leaned against the seat back while the hip was moved to the midpoint of the seat pan. For the posture categories 8 and 9, participants crossed the right (left) leg over the left (right) leg. For the posture categories 10 and 11, participants were instructed to rotate the upper back and shoulder together about 20 degrees according to an external visual reference.

In each trial, the measurements from the twelve sensors were collected at a

sampling frequency of 10Hz, and, their median values were transformed to the corresponding SI units of distance or pressure. For each trial, the distance and pressure values along with the posture category label were recorded. The data collection protocol was approved by the Institutional Review Board of Seoul National University (IRB No. 1605/003-008).

Table 3.2: Participant demographic information

Gender	N	Age[a] (year)	Height (mm)	Weight (kg)
Male	21	26.7±2.0	175.9±6.4	77.1±15.0
Female	15	25.0±2.3	162.8±4.6	51.4±4.3

[a]Mean±Standard deviation

3.2.5 Comparative Evaluation of Posture Classification Performance

The posture classification performance of the mixed sensor system was evaluated in comparison with those of two benchmark systems. The benchmark systems employed only a single type of sensors. They were: the pressure sensors only and the distance sensors only system. This comparative evaluation was aimed at quantifying the effectiveness of combining seatback distance and seat cushion pressure sensors, which was the unique design feature of the mixed sensor system.

The pressure sensors only system chosen for the comparative evaluation consisted of an office chair and an array of six FSRs embedded inside the seat cushion, which were identical to those of the mixed sensor system – in other words, the pressure sensors only system was the same as the mixed sensor system with the distance sensors deactivated. In the same way, the distance sensors only system was identical to the mixed sensor system with the pressure sensors deactivated. Thus, the pressure and distance sensors measurement data contained in the dataset for training and testing the posture classifier of the mixed sensor system (Section 3.2.4) were utilized to build and evaluate the kNN classifier for each of the two benchmark systems - the entire dataset was utilized for the mixed sensor system. The subset of the entire dataset containing the FSR measurement data was utilized for the pressure sensors only system; and, the subset containing the distance sensors measurement data, for the distance sensors only system.

While all of the eleven posture categories were considered in training and testing the classifiers, for each of the left and right posture pairs in Figure 3.1 (posture categories 4 & 5, posture categories 8 & 9, and posture categories 10 & 11), only the left one (posture categories 4, 8 and 10) was considered in describing the performance of the classifiers. In other words, the right postures (posture categories 5, 8 and 11) were removed from the confusion matrices constructed for the three classifiers. This was to avoid double counting identical evaluation results - for each of the three posture category pairs, the classifier performance evaluation results were almost identical for

the left and right postures as the two (left and right) postures as well as the sensor placements were bilaterally symmetric and also the instructions for the two postures were identical except for the asymmetry.

For each of the three systems, the posture classifier performance was evaluated through stratified 10-fold cross-validation. For each system, the corresponding sensor measurement dataset collected from the thirty-six individuals was divided into ten equal-sized partitions. In one iteration of the cross-validation process, the classifier was trained utilizing nine of the partitions as the training dataset, and was validated using the remaining partition as the test dataset. Ten iterations of this procedure were performed, each time using a different partition as the test dataset. The kNN classifier classified a test case (to be classified) utilizing its nearest neighbors within the training dataset – in other words, the test dataset served as an independent, unseen dataset for cross validation.

In order to evaluate the classification performances of the smart chair systems, four performance measures for multi-class classification were employed: overall accuracy, precision, recall, and F1-score. Overall accuracy is the ratio of the number of correctly classified cases to the number of test cases. Precision is the ratio of the number of correctly classified cases to the number of cases labeled by the system as positive. Recall is the ratio of correctly classified cases to the number of positive cases in the data. F1-score is the harmonic mean of precision and recall.

3.3 Results

3.3.1 Model Parameters and Features

For each of the three smart chair systems, the set of model parameters and features trained on the entire dataset collected from the thirty-six individuals is shown in Table 3.3.

Table 3.3: Model parameters and features

System	Number of nearest neighbors	Feature (weight)
Pressure sensors only	9	P1 & P4 (0.20), P2 & P5 (0.14), and P3 & P6 (0.15)
Distance sensors only	5	D1 & D4 (0.19), D2 & D5 (0.16), and D3 & D6 (0.15)
Mixed sensor	3	P1 & P4 (0.16), P2 & P5 (0.07), D2 & D5 (0.06), D1-D3 & D4-D6 (0.14), and D1-D4 (0.15)

3.3.2 Posture Classification Performance

For each of the three smart chair systems, the normalized confusion matrices for the 10-fold cross validation results is provided in Figure 3.4(a)-(c). Each confusion matrix was normalized by the number of cases in each class - sum of the values in a column is equal to one. The overall accuracies of the pressure sensors only, distance sensors only and mixed sensor systems were 0.59, 0.82 and 0.92, respectively. Figure 3.5(a) provides the mean precision values of the three smart chair systems for each posture category. Similarly, Figure 3.5(b) and 5(c) provide mean recall and mean F1-score values.

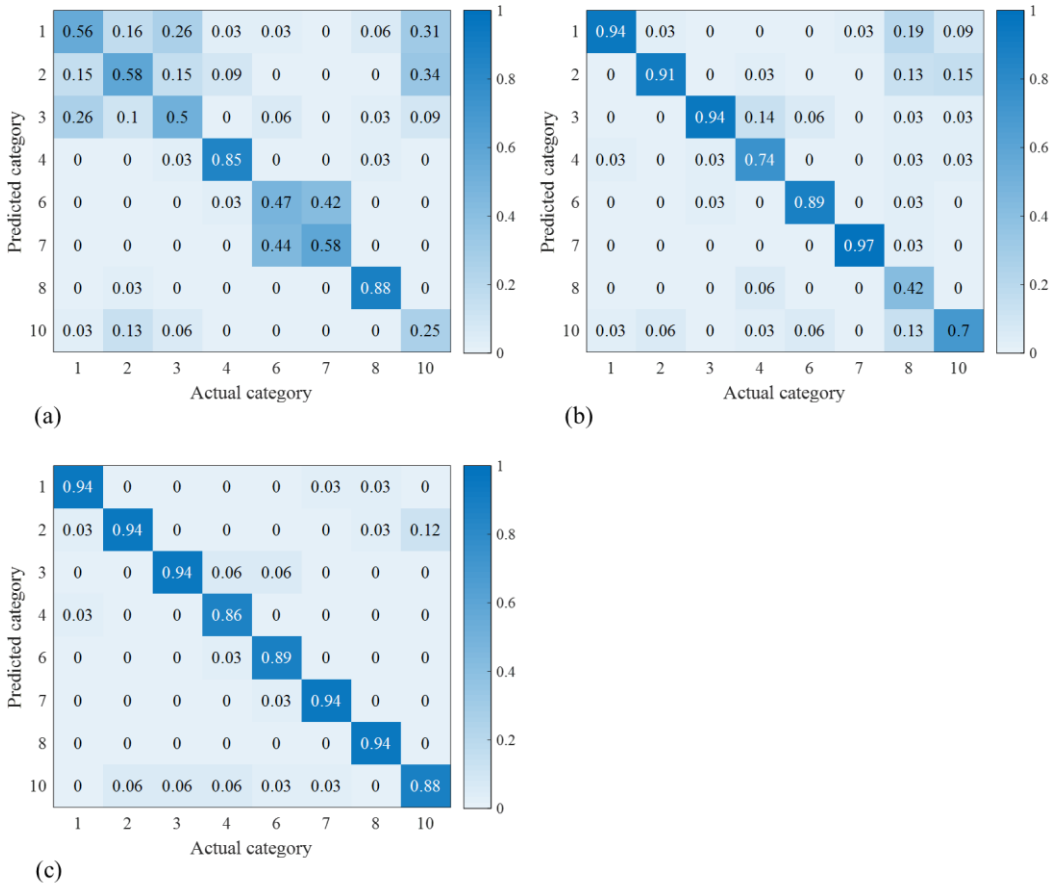

Figure 3.4: The confusion matrices of the posture classification results: (a) the pressure sensors only system, (b) the distance sensors only system, and (c) the mixed sensor system

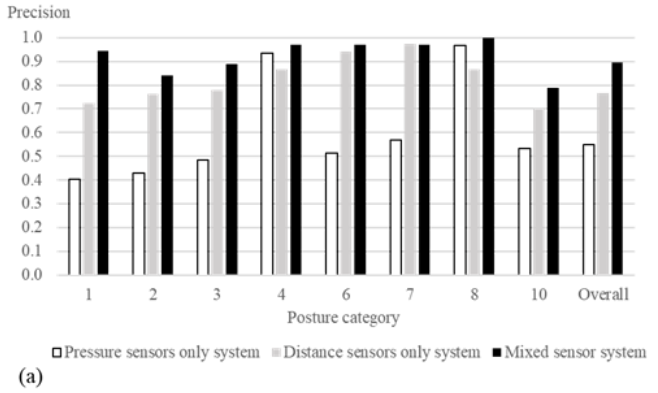

(a)

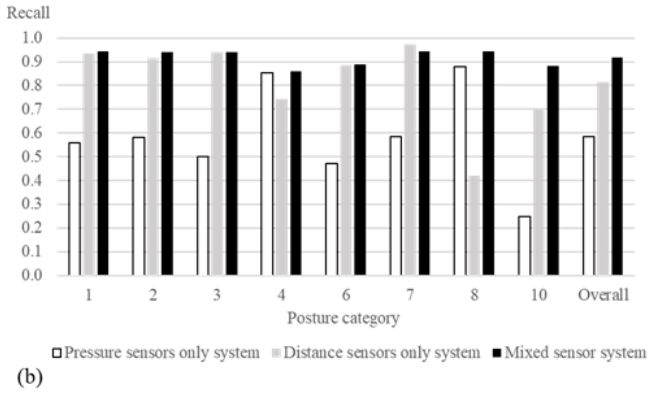

(b)

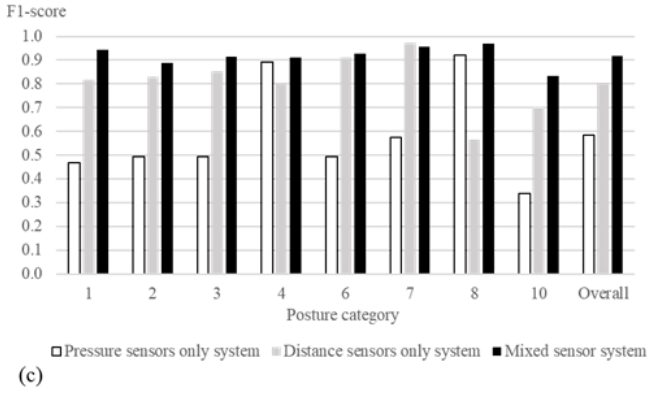

(c)

Figure 3.5: Posture classification performance of the three smart chair systems for each posture category: (a) precision, (b) recall, and (c) F1-score

3.4 Discussion

This study developed a novel mixed sensor smart chair system for monitoring and classifying a worker's sitting postures in real time. The mixed sensor system performed posture classification by combining information from six seat cushion-embedded pressure sensors with that from six seatback-embedded distance sensors. It utilized a kNN algorithm for posture classification - for a given set of sensor measurements, it classified the corresponding posture as one of the eleven predefined posture categories, on the basis of a training dataset. The eleven posture categories were determined based on analyzing the relevant ergonomics literature.

The mixed sensor system was evaluated comparatively against two benchmark systems in posture classification performance. The benchmarks were: the pressure sensors only and distance sensors only systems. They were identical to the mixed sensor system except that they employed only a single type of sensors. An independent, unseen test dataset was utilized for the comparative evaluation.

The mixed sensor system was found to achieve a high overall posture classification accuracy (0.92). On the other hand, the overall accuracies of the pressure sensors only and the distance sensors only system were much lower – they were only 0.59 and 0.82, respectively. Also, it was found that the mixed sensor system was able to perform accurate classifications robustly across all of the posture categories considered (Figure 3.4 and Figure 3.5) - the F1-score of the mixed sensor system ranged

from 0.83 to 0.97 (Figure 3.5(c)). Its performance was better than or comparable to those of the benchmarks consistently across the posture categories considered (Figure 3.5).

The excellent posture classification performance of the mixed sensor system observed in this study is thought to result from combining the two types of sensors - the two sensor types seem to be complementary. In what follows, the impacts of the sensor combination are described focusing on the limitations of the pressure sensors and the roles of the distance sensors.

The mixed sensor system showed far more accurate classification performance than the pressure sensors only system for posture category 10 labeled "Rotating the trunk and keeping the trunk erect." Recall for the posture category 10 was 0.88 and 0.25, respectively (Figure 3.5(b)). The poor performance of the pressure sensors only system is thought to result from the fact that in the upright sitting posture, trunk rotation around the vertical axis by itself does not affect the position of the upper body center of mass (CoM) position or its projection on the seat cushion surface. Therefore, the pressure sensors alone cannot detect or differentiate trunk axial rotations. The distance sensors embedded in the seat back, on the other hand, provide information directly reflecting trunk axial rotations; thus, combining them with the pressure sensors results in improved posture classification performance.

The mixed sensor system was far superior to the pressure sensors only system

in differentiating posture categories 1, 2 and 3, and, posture categories 6 and 7 for which different degrees of trunk flexion account for much of the differences (Figure 3.4(a) and 4(c)). The result seems to reflect the difficulties in differentiating different trunk configurations using only the pressure sensor measurements. One possible scenario in which the pressure sensor measurements would not be able to differentiate trunk configurations is when the back of the thighs does not make a full contact with the seat cushion surface and the weight of the upper body is concentrated on a small area around the ischial tuberosities. For example, if the back of the thighs does not make a contact with the pressure sensors embedded in the front and middle parts of the seat cushion ("P2", "P3", "P5" and "P6"), then the pressure would be concentrated on the rear part of the seat cushion ("P1" and "P4") regardless of trunk configuration. In such situation, only the distance sensors embedded in the seat back would provide information useful for discerning different degrees of trunk flexion.

Another reason why the pressure sensors only system could not accurately classify different trunk configurations is the redundant degrees of freedom of the spinal column. The spinal column consists of twenty-three intervertebral discs with each joint having six degrees of freedom. Consequently, different spinal curvatures may result in the same CoM projections on the seat cushion surface and the same seat cushion pressure distributions. Therefore, the CoM projection alone is not enough to determine the spinal curvature or differentiate different trunk configurations due to trunk flexion or axial trunk rotation, and, neither are the pressure sensor measurements. Again, the

distance sensors are free from this problem and reflect the curvature of spine in a relatively direct manner.

The impacts of the sensor combination could also be described in terms of the roles of the pressure sensors, in other words, how they complemented the distance sensors only system. One observation concerning the distance sensors only system was that it did not accurately classify posture category 10 (labeled "Rotating the trunk and keeping the trunk erect"). Recall for posture category 10 was only 0.7 (Figure 3.4 and Figure 3.5). This is possibly because 1) left trunk rotation occurred simultaneously with some trunk flexion due to the interference between the left shoulder and the seatback, and 2) some participants did not sit exactly in the center of the seat cushion. Sitting off the center of the seat cushion could made deviations of the distance sensor measurements and worsen classification performance. The pressure sensor measurement data may have captured and contributed to correcting such offsets.

The distance sensors only system showed relatively better performance than the pressure sensors only system except for posture category 8 labeled "Legs crossed." For posture category 8, recall of the distance sensors only system was only 0.42 while that of the pressure sensors only system was 0.88 (Figure 3.4 and Figure 3.5). This is not surprising, as the distance sensors could not provide information about the user's leg posture. It is thought that the information from the pressure sensors complemented that from the distance sensors to correctly portray posture category 8 "Legs crossed."

It may be worth providing some discussion on the hyperparameters of the kNN classifiers. First, regarding the results on the hyperparameter k (the number of nearest neighbors of a kNN algorithm), the optimal k value was the smallest for the mixed sensor system; and, between the two benchmark systems, it was smaller for the distance sensors only system than for the pressure sensors only system (Table 3.3). In general, the optimal k value of a kNN classifier is known to increase as the boundaries between the classes become less obvious [100]. The observation is thought to confirm the strength of the design strategy combining the two types of sensors.

Second, for each smart chair system considered in this study, the feature weights help determine the relative importance of the sensors located at different locations [95], [96], [101]. As shown in Table 3.3, the pressure sensor measurements near the hip segment ("P1" and "P4") had larger feature weights than those near the knees ("P3" and "P6") and thighs ("P2" and "P5") in the systems that adopted pressure sensors. This suggests that the pressure sensor measurements of the hip region were more important than the rest. In the mixed sensor system and the distance sensors only system, the uppermost of distance sensor-related feature ("D1-D4") had the largest feature weights among the distance-related features. This implies that the position of the upper part of the trunk played a major role in posture classification. It may be that the sensors involving large feature weights are the targets for design changes when attempting to optimize the sensor placement.

Overall, this pilot study demonstrated the feasibility and utility of a novel, non-invasive, chair-based posture monitoring system, which combined the pressure distribution and the seatback-trunk distances data. The results of the posture classification performance evaluation (Figure 3.4 and Figure 3.5) revealed that: 1) the mixed sensor system was capable of accurately classifying sitting postures robustly across major posture categories that are ergonomically relevant, and, 2) the excellent performance of the mixed sensor system was attributable to the design strategy of combining pressure and distance sensors. The proposed mixed sensor system is considered an improvement over the existing pressure sensor-based smart chair systems in that it enables classifying a wide variety of ergonomically important sitting postures, economically using a small number of sensors.

The mixed sensor system presented in this study may have various applications. The mixed sensor system could be combined with a real-time feedback/warning system to help the users adjust their postures and thereby contribute to reducing the risk of WMSDs. Another possible application of the mixed sensor system currently under our consideration is estimating the seated worker's mental workload from conducting a cognitive task on the basis of real-time posture measurements. Such mental workload estimation could serve as a basis for optimizing job scheduling.

Further research may be conducted to improve the current mixed sensor system. It is expected that posture classification accuracy is affected by the locations

of the pressure and distance sensors [50]. By exploring different sensor placement possibilities, it may be possible to identify new designs that achieve equivalent or enhanced performance with a smaller number of sensors. Also, a future study is warranted to compare the mixed sensor system of the current study against smart chair systems that employ the same number of sensors of a single type, that is, a pressure sensors only system with 12 pressure sensors and a distance sensors only system with 12 distance sensors. Such a study may provide additional information regarding the benefits of combining different types of sensors.

Chapter 4

Severe Obesity Impacts on Joint Kinematics and Movement Technique During Manual Load Lifting

4.1 Introduction

Obesity is a physical condition defined as abnormal or excessive fat accumulation of the body [21]. The body mass index (BMI), calculated as mass/height^2 (unit: kg/m^2), is an indicator of overall adiposity and is moderately correlated with percent body fat [22], [23]. A person is classified as normal-weight if the BMI is greater than 18.5 and less than 25 kg/m^2, pre-obese if it is greater than or equal to 25 kg/m^2 and less than 30 kg/m^2, and obese if it falls within the range of 30 kg/m^2 or higher. The condition of obesity is further subdivided into different categories: obesity class I (30 kg/m^2 $\leq$ BMI $<$ 35 kg/m^2), obesity class II (35 kg/m^2 $\leq$ BMI $<$ 40 kg/m^2), and obesity class III (40 kg/m^2 $\leq$ BMI) corresponding to severe or morbid obesity [25], [102].

Pre-obesity and obesity have increased in the last several decades and are currently prevalent worldwide. From 1975 to 2014, the worldwide prevalence of obesity has increased from 3.2% to 10.9% in men, and from 6.4% to 14.9% in women; if the trends continue, 18% of men and 21% of women are expected to be obese by 2025 [26]. According to the World Health Organization, 1.9 billion adults worldwide were

estimated to be pre-obese or obese in 2016, of which 650 million, or 13% of adults, were obese [21]. Severe obesity also accounts for a nontrivial portion of the global population. For example, in the United States, the prevalence of severe obesity was 7.7% among adults aged 20 years or older in 2015-2016 [27]. The obesity prevalence of the workforce follows that of the general population and obesity rates among various occupational groups increased significantly over time [28]. In the United States workforce, the obesity rate doubled from about 15% to 30% between 1986 and 2011 [29].

Obesity is associated with decreases in work capacity. The presence of excessive adipose tissue adversely affects the capacity of the neuromusculoskeletal system, including joint range of motion, muscle strength, power generation, and reaction time [30]–[37], [103]. Work task design that does not take into account the characteristics of obese workers is thought to be part of the causes of work-related musculoskeletal disorders (WMSDs) in the obese workforce [33], [103], [104]. It may also be related to productivity loss, higher absenteeism, and higher lifetime cost due to disabilities of obese workers [38]–[40].

To alleviate the occupational musculoskeletal problems of obese workers and to improve productivity in the workforce, much research has been conducted on the impacts of obesity on physical loads and task performance during various physical work tasks. Previous studies examined how obesity affects biomechanical loads in manual lifting [64] and carrying [65], movement kinematics of manual lifting [66]–[69], perceived

postural stress during static posture holding [70], functional limitations in reaching [71]–[73], postural stability in manual lifting [74], [75] and quiet standing [76], tolerance limits in manual lifting [70], and reaction time in seated foot reaching [37]. These studies provided implications of their findings concerning the ergonomics work task design for obese workers.

Among the above-mentioned studies, several studies examined the impacts of obesity on manual load lifting [64], [66]–[70]. Manual lifting is one of the important risk factors for low back disorders [78]–[80]. Singh et al. [64] and Corbeil et al. [66] predicted the stresses at the L5/S1 disc joint during manual load lifting by utilizing a biomechanical model and reported that obese individuals had greater lumbar loadings, and, thus, they could be more vulnerable to low back disorders than normal-weight individuals. Colim et al. [69] examined trunk flexion, knee flexion, and pelvis inclination during vertical handling tasks in the presence of a barrier that replicates a typical industrial bin, and the results demonstrated that the obese subjects had greater trunk acceleration and larger horizontal distance between the ankle and the knuckle, suggesting that they were exposed to a higher risk of musculoskeletal disorders (MSDs) development. According to Xu et al. [67], high BMI subjects had significantly higher peak trunk acceleration and velocity when performing free-style dynamic lifting. The authors' hypothesis that obese people might lift slowly to minimize loadings caused by greater body mass and acceleration was not supported by the results. Sangachin and Cavuoto [68] compared the trunk kinematics, heart rate, and task duration of obese

and normal-weight groups when performing prolonged repetitive lifting. When fatigue occurred due to prolonged lifting, trunk acceleration increased in the obese group over time, which was explained in terms of a change in lifting strategy caused by obesity-related characteristics. Singh et al. [70] investigated the psychophysical effects of obesity on lifting tolerance limits and it was found that there was no significant difference in the maximum acceptable weights of lift between the obesity levels.

Despite previous research efforts, however, there still remain knowledge gaps concerning the impacts of obesity on manual load lifting. Especially, little research has been conducted on the impacts of severe obesity (BMI $\geq$ 40 kg/m2) on the way workers organize lifting motion patterns. Although the proportion of individuals with a BMI of 40 or higher in the entire obese population has been gradually increasing [105], and severe obesity has been reported to have a greater impact on the musculoskeletal system than obesity class II or less [106], [107], the authors are not aware of any studies examining the impacts of severe obesity on manual load lifting, except for Singh et al. [64]. Also, the existing studies in general did not analyze lifting motions in terms of multi-joint movement organization or at the level of movement technique.

To address the above knowledge gap, and, contribute to the ergonomics design of lifting tasks, this study aimed to identify the impacts of severe obesity on joint kinematics and movement technique during manual lifting under four different task conditions, and, further provide design information for ergonomic interventions or work

task design for high BMI individuals.

4.2 Methods

4.2.1 Participants

Eighteen normal-weight (18.5 kg/m^2 ≤ BMI < 25 kg/m^2) and 17 severely obese (BMI ≥ 40 kg/m^2) participants participated in this study. Individuals without a history of severe low back disorder and other obvious musculoskeletal disorders were considered in the study. The demographic information of the participants is summarized in Table 4.1.

Table 4.1: Summary of participants' demographic information.

	Non-obese (n=18)	Obese (n=17)	p value
Age (years)	28.00 (6.62)	28.92 (7.99)	0.768
Height (m)	173.36 (7.89)	168.65 (11.35)	0.157
Weight (kg)	67.85 (15.90)	134.78 (33.32)	<0.001
BMI (kg/m^2)	22.61 (5.09)	47.17 (8.93)	<0.001

4.2.2 Experimental Task

The participants performed low-lying box lifting with box weights equal to the recommended weight limits (RWLs) calculated by the revised National Institute for Occupational Safety and Health (NIOSH) lifting equation. The revised NIOSH lifting equation was developed to determine the limit of hand load weight (that is, RWL) for a given task condition, which could be lifted without an increased risk of developing lifting-related musculoskeletal disorders [77]. Lifting with a weight less than the RWL is known to result in an L5/S1 disc compressive force less than 3400N, which is considered safe for most healthy workers [77].

A total of four lifting task conditions were considered in this study, all of which were sagittally symmetric. The origins of the four lifting task conditions were identical, and the destinations were determined by combining two levels of horizontal location with two levels of vertical location (Table 4.2). The horizontal location of the load was defined as the horizontal distance between the midpoint of both the ankle joints and the box center, and the vertical location was determined as the vertical distance from the ground to the box handle (Figure 4.1(a)). These locations were part of the task parameters of the revised NIOSH lifting equation. The origin and the destination of each lift were created using wooden slabs and a height-adjustable shelf (Figure 4.1(b)). For each task condition, the box weight (the RWL) was calculated using the revised NIOSH lifting equation. See Waters et al. [77] for detailed descriptions of the parameters of the revised NIOSH lifting equation and the RWL calculation.

Table 4.2: Lifting task conditions

Task Condition	Origin		Destination		Box weight (kg)
	Horizontal location (m)	Vertical location (m)	Horizontal location (m)	Vertical location (m)	
1	0.33	0.18	0.66	1.05	12.6
2			0.66	1.52	12.3
3			0.75	1.05	12.6
4			0.75	1.52	12.3

Note: as for the other parameters of the revised NIOSH lifting equation, the coupling quality and the lifting frequency were 'good' and 'infrequent' (<0.1 lift per minute) for the work duration of less than 1 hour, respectively, and, the angle of asymmetry was zero in all of the four lifting task conditions.

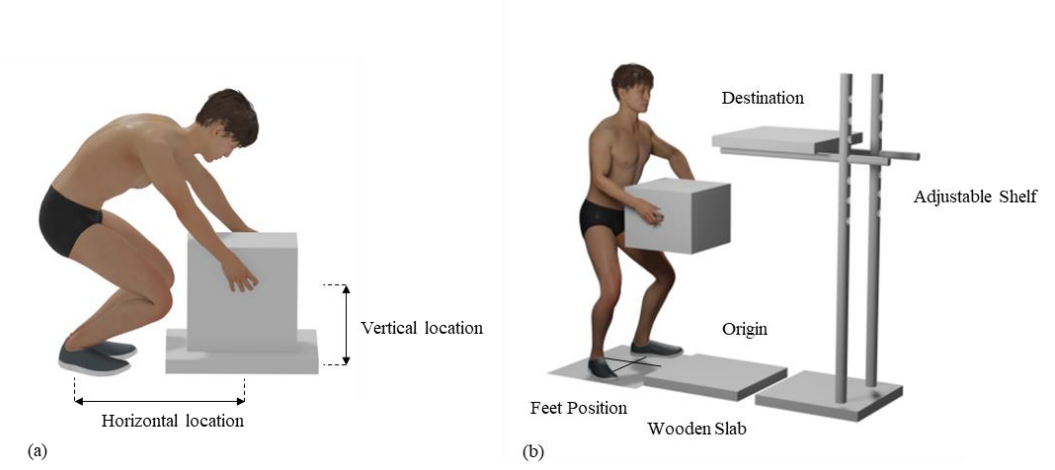

Figure 4.1: Experimental setup: (a) Horizontal and vertical location at the origin, (b) Illustration of the lifting task.

4.2.3 Experimental Procedure

In this study, a lifting motion in each trial was recorded using a twelve-camera Vicon motion capture system (Vicon, Oxford, UK), sampled at 120Hz using a Vicon Nexus software. Prior to the experimental session, for each participant, a set of optical markers were placed on the specific body anatomical landmarks according to the Plug-in-Gait model of the Vicon motion capture system [108].

For some of the severely obese participants, excessive fat in the abdomen occluded or distorted the positions of the markers on the front waist (the right and left anterior superior iliac spine [ASIS] markers) necessary to define the pelvis segment. This caused difficulties in properly estimating the positions of the hip joint centers, which were the outputs of the Plug-in-Gait model. To solve the problem, the following measures were taken: first, each participant was laid on a flat surface, and the experimenter palpated the ASIS bony landmarks. The distance between the two bony landmarks was measured using a pair of calipers - this distance was used to estimate the positions of the hip joint centers based on the Plug-in-Gait model. Second, the ASIS markers were moved laterally outward from the ASIS bony landmark positions by an equal amount, along the right-left ASIS axis found through the palpation. This was to avoid the marker occlusion by the abdominal fat and make the markers visible to the cameras during the lifting task trials. The marker position adjustments did not affect the coordinate system of the pelvis segment and thus the estimation of the

positions of the hip joint centers based on the Plug-in-Gait model. The markers attached to the other anatomical landmarks (e.g., knee, shoulder) did not cause the problem of occlusion by body fat for the severely obese participants.

During each lifting trial, each participant was standing on the marked feet position with minimal flexion of upper and lower extremities, and with a start signal, the participant began the movement. The participant grabbed the box at the origin of the lift, lifted it using a self-selected, free-style lifting technique, and placed the box at the destination of the lift. Each participant performed a single trial for each of the four lifting task conditions. The order of the trials was randomized for each participant, and sufficient rest time was given between consecutive trials. The experimental protocol was approved by a local Institutional Review Board.

4.2.4 Data Processing

Since the lifting task conditions were sagittally symmetric, the participants were represented by the kinematic chain shown in Figure 4.2. The lifting movements were characterized by the flexion-extension angles of the following joints: ankle, knee, hip, spine, shoulder, and elbow. Note that the inclination of the pelvis segment was calculated by the positions of the waist markers, that is, the anterior and posterior superior iliac spine markers (the ASIS and PSIS markers), and the hip and the spine angle were defined as the relative angle between the pelvis and the thigh segment, and,

that between the pelvis and the thorax segment, respectively.

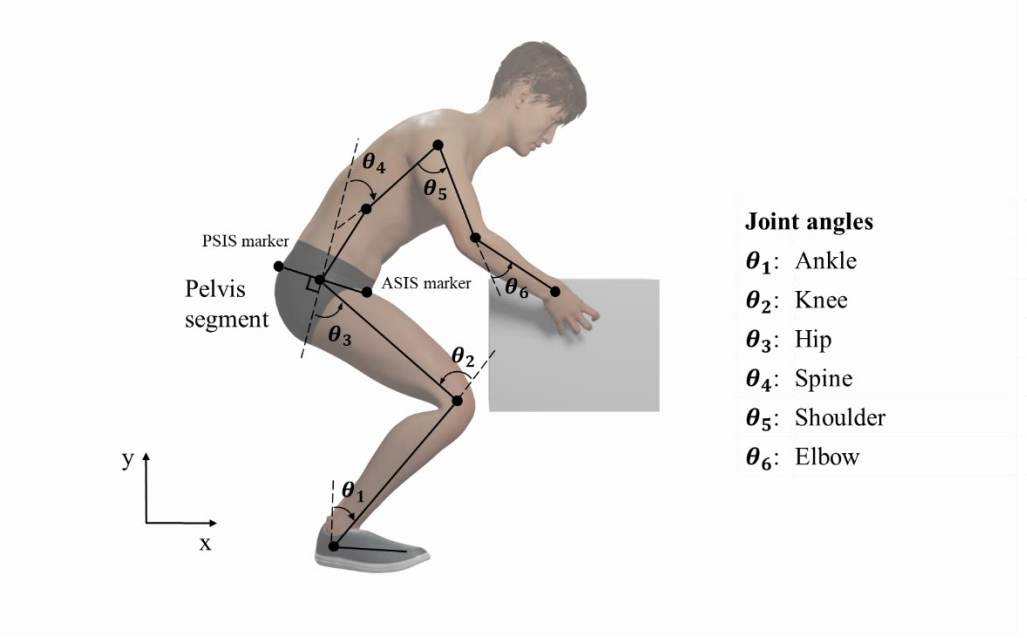

Figure 4.2: Six-segment, six-angle kinematic chain representing the human body in the sagittal plane

In each lifting trial, the trajectories of the optical markers were recorded, and both the position- and the angle-time trajectory of each joint were calculated by the Plug-in-Gait model (Figure 4.3). In this study, we analyzed each participant's movement while the box moved from the origin to the destination of the lift. The outputs of the model were filtered using a fourth-order Butterworth low-pass filter with a cut-off frequency of 3Hz. All data processing was conducted using Vicon 2.11.0 and

Matlab R2020b.

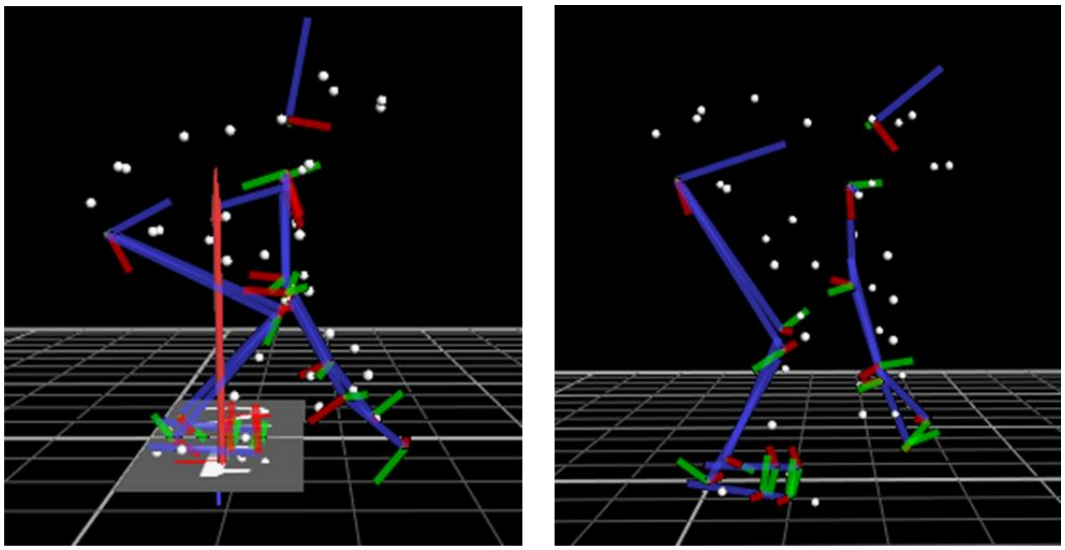

(a) Non-obese participant (b) Severely obese participant

Figure 4.3: Example of recording the optical markers in a lifting trial for each participant group: (a) Non-obese participant and (b) severely obese participant

4.2.5 Experimental Variables

The independent variables of this study were Obesity Level (normal-weight and obese) and Task Condition (four load destinations). The dependent measures were a set of kinematic variables and two movement technique indexes derived from the joint angle trajectories.

The kinematic variables were the duration of movement and the joint range of

excursion (ROE), the mean of absolute joint angular velocity, and the peak joint angular acceleration at each body joint. These kinematic variables were obtained from the joint angle-time trajectory as the box moved from the origin to the destination of the lift. For each lifting trial, the duration was defined as the time from the moment the box leaves the origin to the moment it arrives at the destination. The ROE was defined as the difference between the maximum and the minimum angle for each joint. The mean absolute angular velocity and peak angular acceleration were determined from the joint angular velocity and acceleration trajectories, which were calculated with numerical differentiation.

The movement technique of a lifting trial could be characterized on the basis of the posture (joint angles) adopted at the start of the lift. Burgess-Limerick and Abernethy [109] proposed a postural index to quantify the lifting techniques from stoop to squat. Postural index was defined as the ratio of knee flexion to the sum of the ankle, hip, and spine flexion at the start of a lift (Equation 4.1 and Figure 4.2). When the knee flexion from the normal standing position is small and the forward inclination of the trunk is large, postural index approaches zero and describes that the lifting technique is closer to a stoop than to a full squat (Figure 4.4(b)). Conversely, postural index of close to one suggests that the participant adopted a squat technique with high knee flexion and low trunk inclination (Figure 4.4(a)). Postural index was empirically shown to be robust to changes in task parameters such as the vertical location of origin and load weight [109].

$$postural\ \ index = \frac{knee\ \ flexion\ (°)}{ankle+hip+spine\ \ flexion\ (°)} \tag{4.1}$$

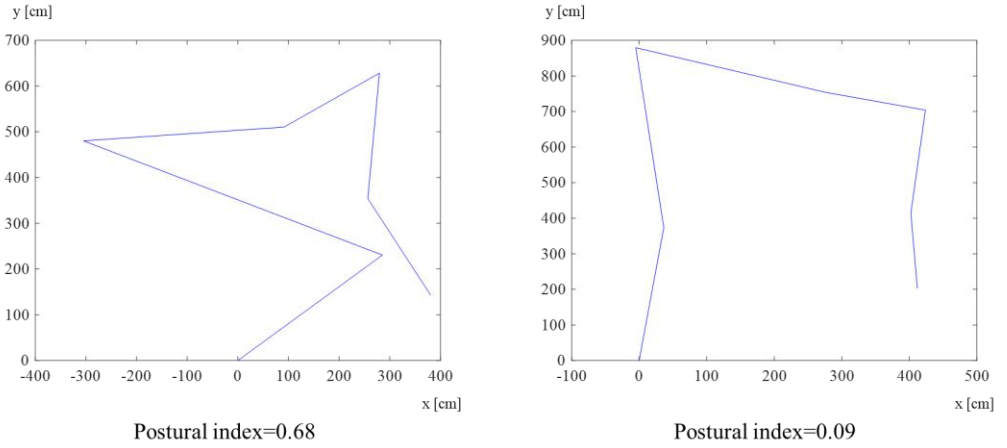

(a) Lifting technique close to the squat (b) Lifting technique close to the stoop

Figure 4.4: Examples of postural indexes according to lifting techniques

The other movement technique index utilized in this study was the joint contribution vector (JCV) index proposed by Park et al. [110] to characterize goal-directed motions in movement technique. The JCV index represents the movement technique underlying a goal-directed motion in terms of the relative contributions of the individual joint degrees of freedom (DOFs) to the end-effector (e.g., hand) trajectory formation. The individual joint contributions constituting the JCV were utilized as dependent measures.

The following are the details of calculating the JCV index. A discrete, goal-

directed human motion is defined as a set of joint angle-time trajectories with N DOFs during a time interval t ∈ [0, T] (Equation 4.2). The contribution of the ith joint DOF could be assessed by comparing the motion with an "almost identical" motion in Equation 4.3 that eliminates (freezes) the ith joint DOF in the motion (Figure 4.5). The x-axis component of the contribution of the ith joint DOF is defined as Equation 4.4, where $x(t)$ and $x^i(t)$ are the x-coordinates of the end-effector corresponding to $\boldsymbol{\theta}(t)$ and $\boldsymbol{\theta}^i(t)$, respectively. The contribution of the ith joint DOF in the x-axis could be further normalized to the percent contribution (PC) ranging from -100 to 100 (Equation 4.5). Likewise, the contribution of the ith joint DOF in the y-axis is calculated and normalized as Equations 4.4 and 4.5. In this study, the lifting motions in the sagittal plane were characterized by the JCVs with the horizontal (JCV_x) and vertical (JCV_y) components (Equation 4.6).

$$\boldsymbol{\theta}(t) = [\theta_1(t) \dots \theta_i(t) \dots \theta_N(t)] \tag{4.2}$$

$$\boldsymbol{\theta}^i(t) = [\theta_1(t) \dots \theta_i(0) \dots \theta_N(t)] \tag{4.3}$$

$$C_x^i = \int_0^T \left(x(t) - x^i(t)\right) dt \,, C_y^i = \int_0^T \left(y(t) - y^i(t)\right) dt \tag{4.4}$$

$$PC_x^i = \frac{100 \times C_x^i}{\sum_{j=1}^{N} \left|C_x^j\right|}, PC_y^i = \frac{100 \times C_y^i}{\sum_{j=1}^{N} \left|C_y^j\right|} \tag{4.5}$$

$$\mathbf{JCV_x} = \left[PC_x^1 \dots PC_x^i \dots PC_x^N\right], \mathbf{JCV_y} = \left[PC_y^1 \dots PC_y^i \dots PC_y^N\right] \tag{4.6}$$

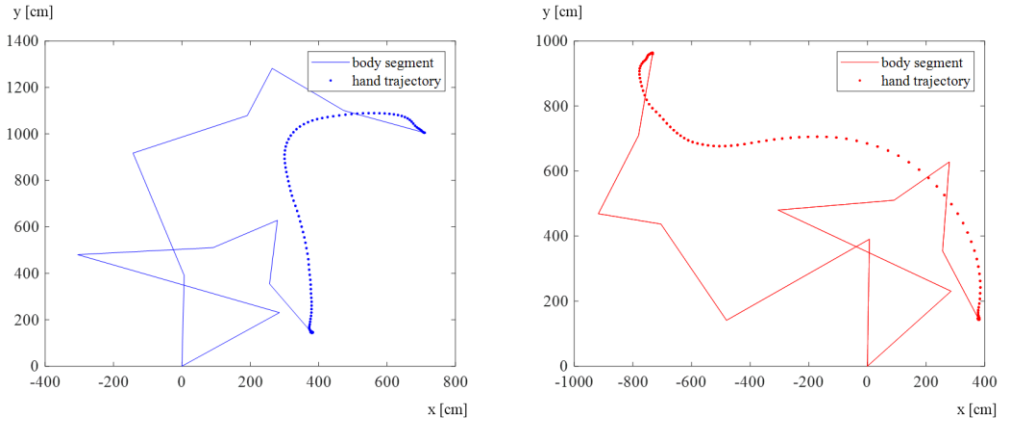

(a) Lifting motion

(b) "Almost identical" lifting motion that eliminates the knee joint DOF

Figure 4.5: Example of a lifting motion and "almost identical" motion that eliminates the knee joint DOF.

4.2.6 Statistical Analysis

The experiment was based on the design with the between-subject factor of Obesity Level (two levels; normal-weight and obese) and the within-subject factor of Task Condition (four levels). For each dependent measure, a series of two-way mixed ANOVAs were conducted to test the effects of Obesity Level, Task Condition, and their interaction on each of the dependent variables. Prior to analysis, the assumption of independent observations, normality of residuals, and homogeneous variance of

residuals was tested using the approaches proposed by Montgomery [111]. In the case of violation of the homogeneous variance or normality assumption, natural log transformation was applied to those dependent variables, and the transformation remedied the violation. The sphericity assumption of repeated-measures ANOVA was tested using Mauchly's sphericity test, and Greenhouse-Geisser correction was applied in case of a violation. Post hoc analyses using the Tukey HSD test were conducted for the dependent variables if the main or interaction effects were significant. Statistical significance was set at $p < .05$. Analyses were conducted using the R statistical software, version 3.5.1.

4.3 Results

4.3.1 Kinematic Variables

The statistical analysis results for the kinematic variables are summarized in Tables 4.3-4.6. Obesity Level and Task Condition was found to have significant effects on the duration (Table 4.3 and Figure 4.6). None of the interactions were found to be significant for the duration (Table 4.3).

Obesity Level was found to have significant effects on the ROEs of the ankle, knee, hip, and elbow joints (Table 4.4 and Figure 4.7). Task Condition showed a significant effect on the ROEs of all joints (Table 4.4 and Figure 4.7). The Obesity

Level × Task Condition interaction effects were significant for the ROE of the ankle joint (Table 4.4 and Figure 4.10(a)).

As shown in Table 4.5 and Figure 4.8, Obesity Level had a significant effect on the mean absolute angular velocity for all joints except the spine joint, and Task Condition was found to have significant effects on the mean absolute angular velocity for all joints. The Obesity Level × Task Condition interaction effects were significant on the mean absolute angular velocity of the ankle and knee joints (Table 4.5 and Figure 4.10(b) and 4.10(c)).

Obesity Level significantly affected the peak angular acceleration of the knee and elbow joints, and Task Condition significantly affected that of the spine, shoulder, and elbow joints (Table 4.6 and Figure 4.9). None of the interactions were found to be significant for the peak angular acceleration (Table 4.6).

Table 4.3: Summary of descriptive statistics and ANOVA results for the duration.

	Task condition 1		Task condition 2		Task condition 3		Task condition 4		*p*-values		
	Normal-weight	Obese	Normal-weight	Obese	Normal-weight	Obese	Normal-weight	Obese	Obesity Level	Task Condition	Interaction
Duration (s)											
	2.41 (0.35)	2.67 (0.69)	2.59 (0.26)	3.04 (0.66)	1.98 (0.32)	2.26 (0.4)	2.36 (0.34)	2.75 (0.57)	0.026	<0.001	0.321

Note: Means and standard deviations are provided for descriptive statistics (standard deviations are presented in parentheses). Significant p-values are in bold.

Table 4.4: Summary of descriptive statistics and ANOVA results for the range of excursion.

	Task condition 1		Task condition 2		Task condition 3		Task condition 4		*p*-values		
	Normal-weight	Obese	Normal-weight	Obese	Normal-weight	Obese	Normal-weight	Obese	Obesity Level	Task Condition	Interaction
Range of excursion (°)											
Ankle	34.6 (8.39)	31.02 (12.09)	31.42 (9.3)	25.15 (17.11)	36.39 (10.64)	22.44 (13.88)	34.06 (8.97)	20.35 (12.01)	0.014	0.008	0.003
Knee	94.13 (23.35)	67.48 (27.85)	90.79 (21.42)	57.99 (32.16)	89.01 (22.73)	47.94 (31.4)	92.4 (19.74)	50.23 (31.21)	<0.001	0.002	0.064
Hip	88.22 (10.79)	69.03 (13.55)	101.73 (10.96)	81.79 (17.82)	81.42 (10.94)	61.98 (16.58)	97.3 (11.93)	76.07 (16.82)	<0.001	<0.001	0.867
Spine	25.32 (6.93)	25.66 (7.06)	38.87 (8.42)	34.41 (8.25)	23.91 (6.37)	23.24 (5.39)	35.82 (8.31)	33.53 (6.42)	0.45	<0.001	0.056
Shoulder	87.31 (12.61)	72.45 (14.63)	99.22 (12.77)	90.29 (17.39)	86.99 (12.38)	84.74 (21.58)	103.37 (16.84)	91.75 (15.38)	0.053	<0.001	0.066
Elbow	71.1 (9.82)	55.26 (10.31)	89.42 (8.57)	78.84 (11.07)	70.02 (11.14)	58.3 (10.66)	88.52 (8.16)	75.05 (9.66)	<0.001	<0.001	0.376

Note: Means and standard deviations are provided for descriptive statistics (standard deviations are presented in parentheses). Significant p-values are in bold.

Table 4.5: Summary of descriptive statistics and ANOVA results for the mean absolute angular velocity.

	Task condition 1		Task condition 2		Task condition 3		Task condition 4		*p*-values		
	Normal-weight	Obese	Normal-weight	Obese	Normal-weight	Obese	Normal-weight	Obese	Obesity Level	Task Condition	Interaction
Mean absolute angular velocity (°/s)											
Ankle	14.58 (4.01)	12.42 (3.86)	12.23 (3.92)	8.83 (5.35)	17.95 (5.75)	10.88 (5.71)	14.3 (4.14)	8.28 (4.43)	0.004	<0.001	<0.001
Knee	42.4 (13.49)	26.9 (15.78)	37.53 (11)	19.17 (11.94)	48.17 (19.29)	21.81 (13.92)	40.68 (11.04)	18.8 (11.9)	<0.001	<0.001	0.041
Hip	38.97 (7.1)	29.99 (8.01)	41.67 (6.12)	29.94 (9.51)	44.62 (7.7)	32.54 (10.39)	45.43 (8.66)	31.25 (10.46)	<0.001	<0.001	0.083
Spine	11.04 (2.82)	10.46 (3.94)	15.61 (3.44)	12.33 (4.36)	12.8 (3.71)	11.12 (3.07)	16.13 (4.39)	13.28 (4.26)	0.112	<0.001	0.132
Shoulder	50.7 (9.69)	40.41 (11.74)	49.03 (7.85)	37.1 (10.96)	52.79 (10.93)	47.66 (11.42)	51.07 (11.03)	40.66 (12.37)	0.003	<0.001	0.81
Elbow	49.2 (9.1)	37.31 (9.71)	62.19 (7.65)	47.87 (10.2)	59.39 (12.78)	47.19 (12.43)	69.9 (8.88)	51.05 (11.4)	<0.001	<0.001	0.402

Note: Means and standard deviations are provided for descriptive statistics (standard deviations are presented in parentheses). Significant p-values are in bold.

Table 4.6: Summary of descriptive statistics and ANOVA results for the peak angular acceleration.

	Task condition 1		Task condition 2		Task condition 3		Task condition 4		*p*-values		
	Normal-weight	Obese	Normal-weight	Obese	Normal-weight	Obese	Normal-weight	Obese	Obesity Level	Task Condition	Interaction
Peak angular acceleration (°/s²)											
Ankle	101.7 (46.32)	104.1 (38.43)	87.56 (42.26)	64.43 (32.23)	109.29 (50.99)	73.71 (37.29)	96.31 (40.94)	64.06 (34.32)	0.134	0.232	0.208
Knee	310.77 (128.29)	225.62 (180.63)	276.15 (96.7)	142.22 (80.86)	313.35 (149.95)	158.86 (95.64)	291.65 (102.7)	152.03 (102.39)	**0.014**	0.443	0.196
Hip	226.17 (59.9)	183.41 (60.77)	233.9 (56.07)	172.82 (50.71)	281.13 (81.04)	220.46 (80.99)	254.68 (68.85)	181.61 (70.51)	0.639	0.189	0.566
Spine	67.27 (20.8)	71.6 (30.61)	91.75 (25.52)	74.89 (28.66)	89.28 (35.29)	79.28 (28.83)	94.97 (36.14)	90.25 (28.29)	0.447	**0.027**	0.844
Shoulder	486.66 (77.59)	288.87 (101.29)	403.69 (101.77)	280.6 (99.72)	558.71 (117.48)	414.16 (135.09)	465.5 (117.97)	350.47 (115.82)	0.264	**<0.001**	0.512
Elbow	440.95 (90.52)	298.64 (99.39)	440.36 (111.06)	331.52 (90.86)	582.52 (130.8)	381.41 (129.03)	559.12 (114.16)	372.19 (108.29)	**0.001**	**<0.001**	0.936

Note: Means and standard deviations are provided for descriptive statistics (standard deviations are presented in parentheses). Significant p-values are in bold.

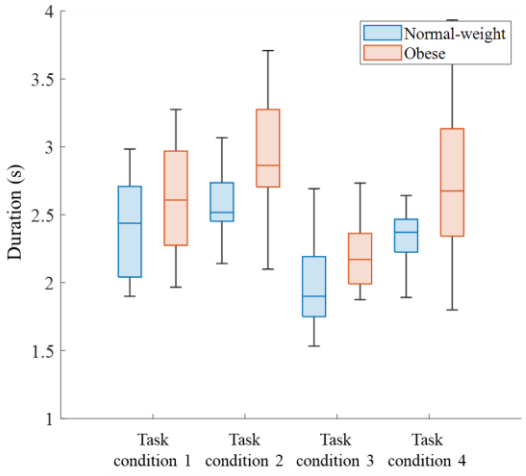

Figure 4.6: Box plots summarizing the duration data for the two obesity levels in each task condition.

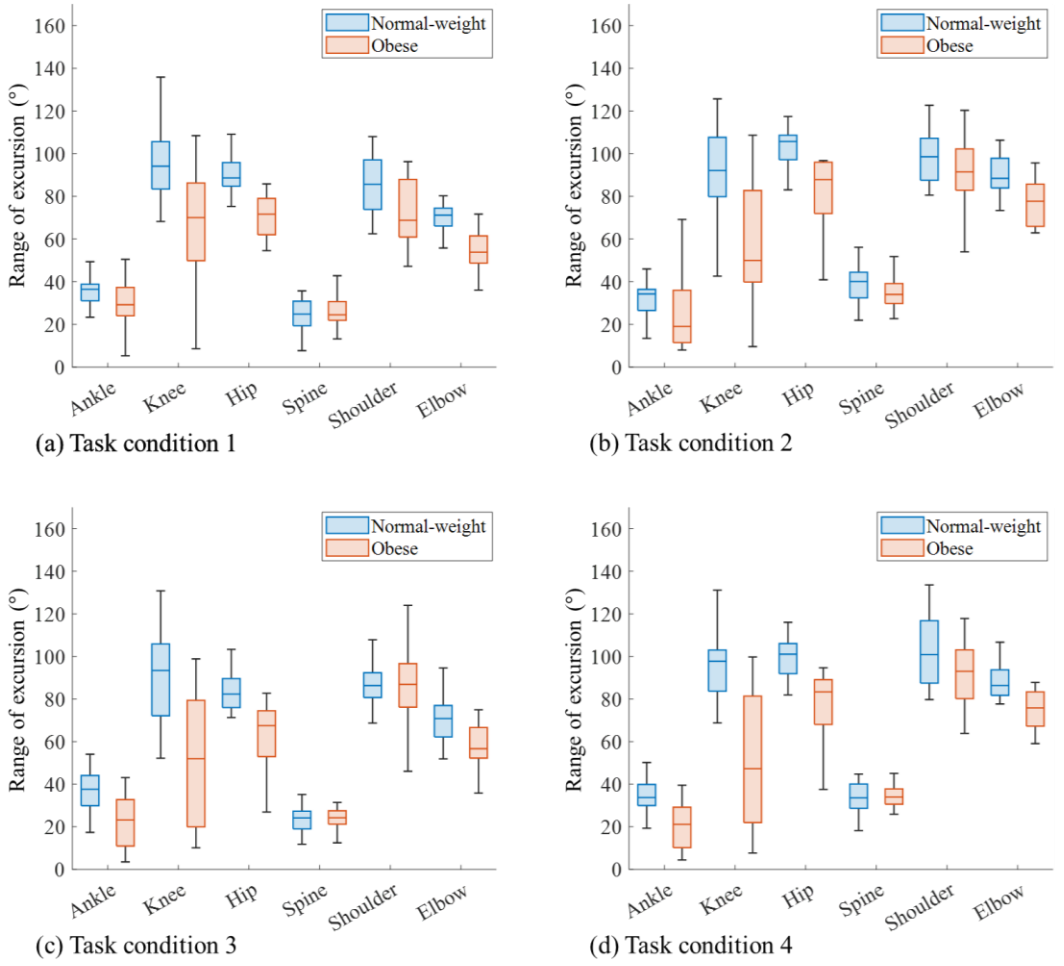

Figure 4.7: Box plots summarizing the range of excursion data for the two obesity levels in each task condition.

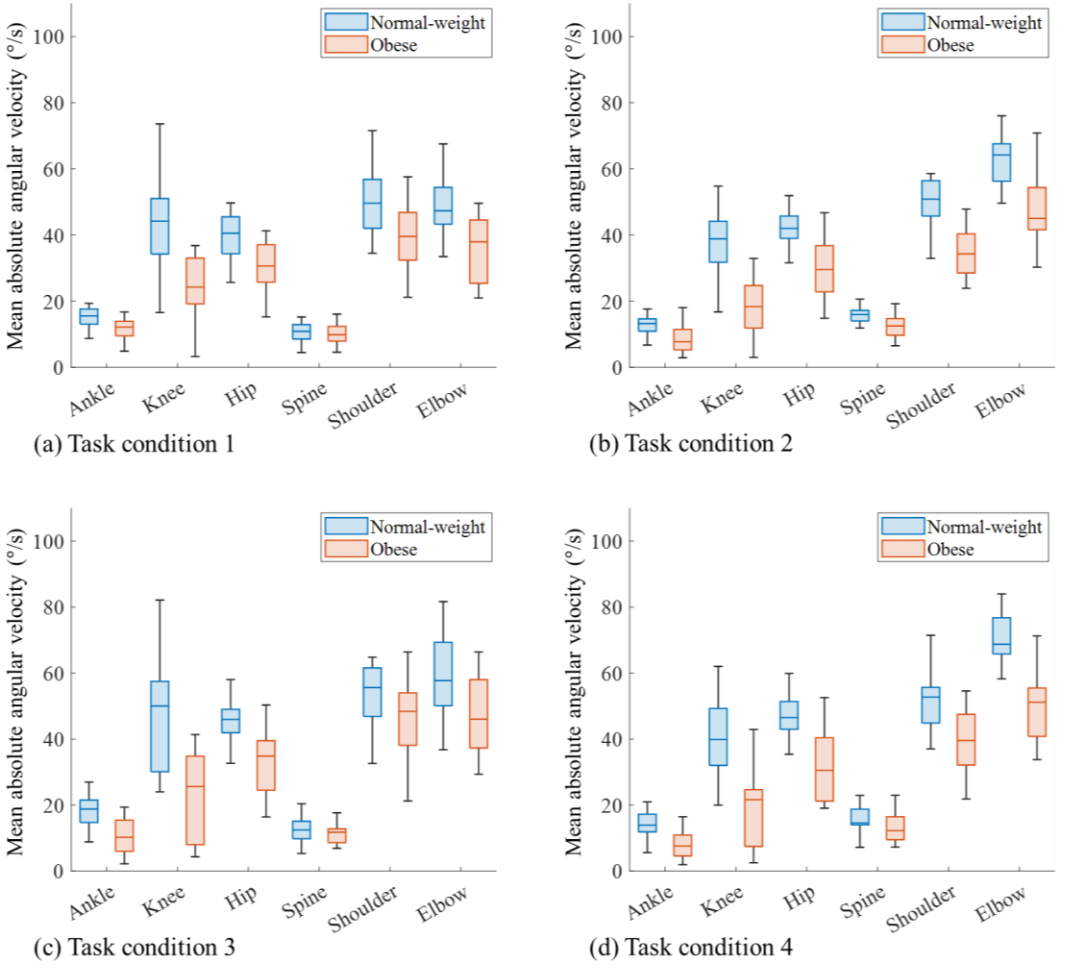

Figure 4.8: Box plots summarizing the mean absolute angular velocity data for the two obesity levels in each task condition.

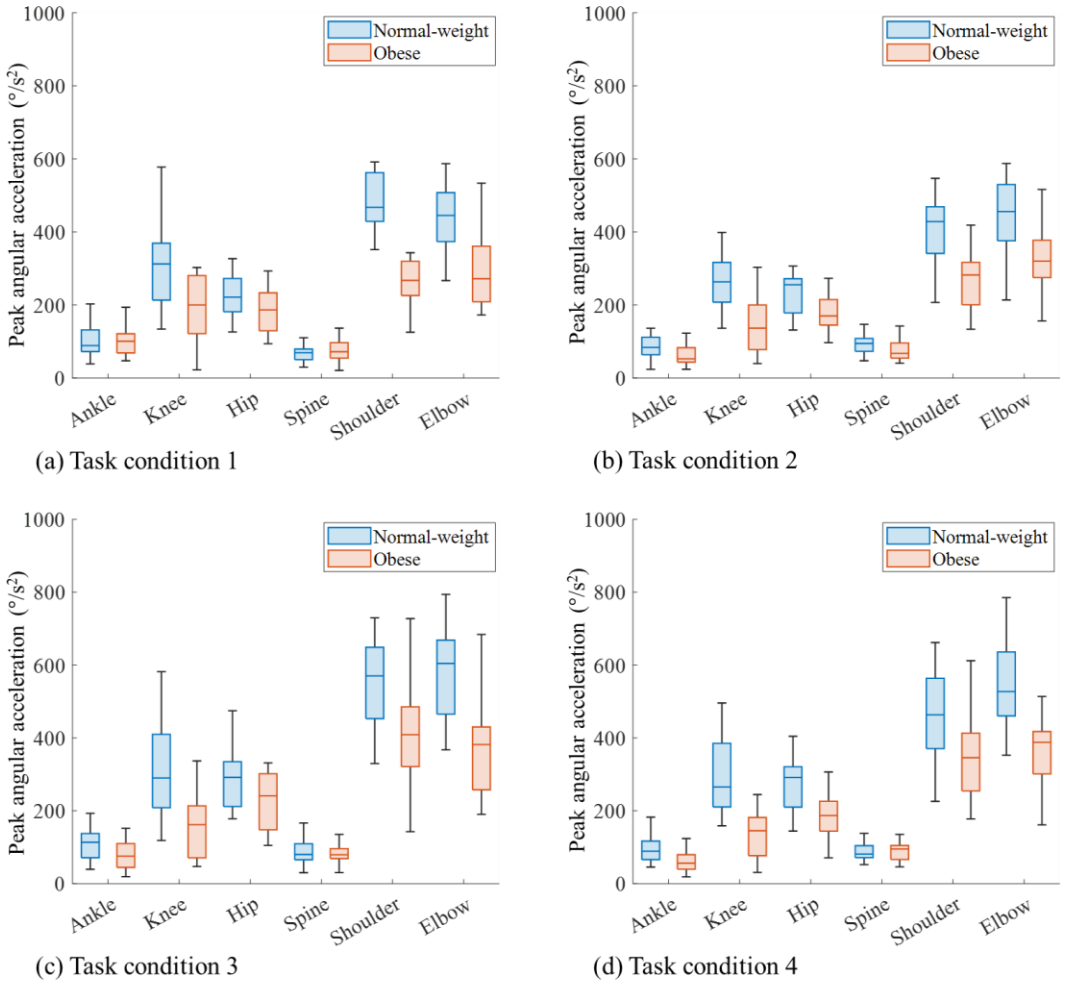

Figure 4.9: Box plots summarizing the peak angular acceleration data for the two obesity levels in each task condition.

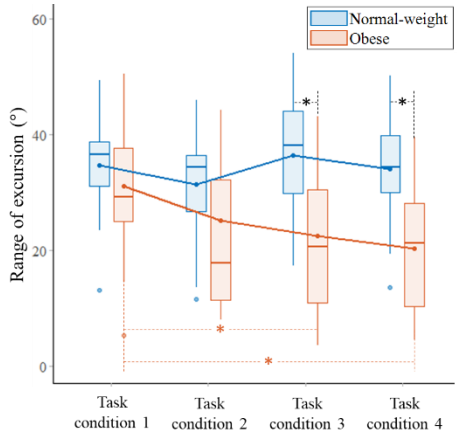

(a) ROE of the ankle joint

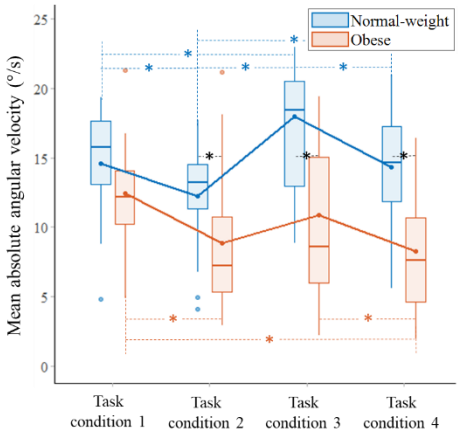

(b) Mean absolute angular velocity of the ankle joint

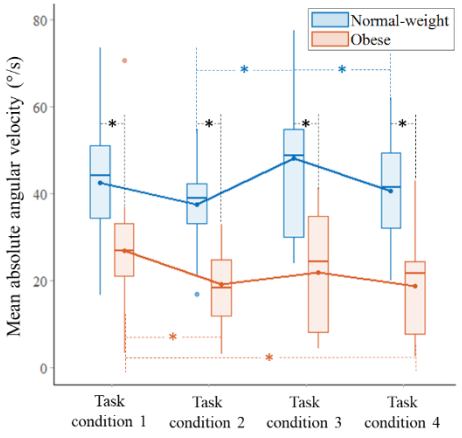

(c) Mean absolute angular velocity of the knee joint

Figure 4.10: Obesity Level × Task Condition interaction effects on kinematic variables: (a) the ROE of the ankle joint, (b) the mean absolute angular velocity of the ankle joint, and (c) the mean absolute angular velocity of the knee joint. '*' denotes significant pairwise differences on Obesity Level or Task Condition.

4.3.2 Movement Technique Indexes

The statistical analysis results for the movement technique indexes (postural index, JCV_x, and JCV_y) are summarized in Tables 4.7-4.9. Obesity Level, Task Condition, and their interaction were found to have significant effects on postural index (Table 4.7 and Figure 4.10).

Obesity Level showed a significant effect on all the components of JCV_x except for the spine joint and Task Condition except for the knee joint (Table 4.8 and Figure 4.11). The Obesity Level × Task Condition interaction effects were significant for the ankle, hip, and spine joint components of JCV_x (Table 4.8 and Figure 4.14).

Obesity Level had a significant effect on the ankle, knee, spine and elbow joint components of JCV_y, and Task Condition had a significant effect on all the components of JCV_y (Table 4.9 and Figure 4.12). The Obesity Level × Task Condition interaction effects were found to be significant for the ankle, knee, hip, and elbow joints components of JCV_y (Table 4.9 and Figure 4.15).

Table 4.7: Summary of descriptive statistics and ANOVA results for postural index.

	Task condition 1		Task condition 2		Task condition 3		Task condition 4		*p*-values		
	Normal-weight	Obese	Normal-weight	Obese	Normal-weight	Obese	Normal-weight	Obese	Obesity Level	Task Condition	Interaction
Postural index											
	0.59 (0.13)	0.46 (0.21)	0.57 (0.09)	0.36 (0.26)	0.55 (0.11)	0.25 (0.3)	0.56 (0.1)	0.26 (0.29)	**0.001**	**0.006**	**0.037**

Note: Means and standard deviations are provided for descriptive statistics (standard deviations are presented in parentheses). Significant p-values are in bold.

Table 4.8: Summary of descriptive statistics and ANOVA results for JCV_x.

	Task condition 1		Task condition 2		Task condition 3		Task condition 4		*p*-values		
	Normal-weight	Obese	Normal-weight	Obese	Normal-weight	Obese	Normal-weight	Obese	Obesity Level	Task Condition	Interaction
JCV_x (horizontal) components (%)											
Ankle	-22.32 (4.1)	-21.52 (9.31)	-28.83 (4.3)	-14.96 (24.2)	-21.75 (3.83)	-11.34 (18.65)	-27.35 (4.72)	-9.73 (23.48)	0.043	<0.001	0.01
Knee	46.45 (6.84)	40.66 (15.98)	58.33 (3.45)	42.57 (25.35)	47.39 (8.3)	27.94 (26.14)	59.47 (4.82)	34.79 (33.33)	0.009	0.248	0.14
Hip	15.1 (5.1)	9.46 (9.25)	0.08 (6.28)	-9.46 (11.47)	15.04 (6.63)	11.77 (11.08)	2.92 (6.87)	-8.55 (12.53)	0.012	<0.001	0.013
Spine	3.64 (1.71)	6.31 (5.12)	-1.65 (1.59)	-3.26 (2.81)	4.23 (2.21)	9.11 (7.86)	-1.14 (1.69)	-3.33 (3.5)	0.38	<0.001	0.027
Shoulder	-6.58 (3.86)	-11.85 (10.38)	-2.6 (1.46)	-7.57 (9.46)	-5.46 (4.35)	-13.49 (10.45)	-2.5 (1.9)	-11.2 (10.47)	0.004	<0.001	0.263
Elbow	5.88 (2.63)	9.51 (7.94)	3.56 (2.98)	5.78 (5.17)	5.76 (2.39)	11.33 (5.8)	3.69 (3.27)	8.1 (6.72)	0.006	0.002	0.305

Note: Means and standard deviations are provided for descriptive statistics (standard deviations are presented in parentheses). Significant p-values are in bold.

Table 4.9: Summary of descriptive statistics and ANOVA results for JCV_y.

	Task condition 1		Task condition 2		Task condition 3		Task condition 4		*p*-values		
	Normal-weight	Obese	Normal-weight	Obese	Normal-weight	Obese	Normal-weight	Obese	Obesity Level	Task Condition	Interaction
JCV_y (vertical) components (%)											
Ankle	28.71 (8.55)	27.73 (15.18)	18.48 (5.42)	14.06 (13.01)	30.43 (10.12)	16.57 (17.66)	21.71 (5.9)	11.29 (13.17)	0.009	0.001	0.022
Knee	5.25 (11.49)	-4.32 (8.06)	17.31 (9.71)	5.04 (11.37)	-2.06 (10.65)	-5.9 (11.55)	13.97 (8.86)	3.43 (9.51)	0.007	<0.001	0.029
Hip	36.26 (3.93)	34.05 (6.66)	41.52 (6.66)	44.16 (10.85)	36.66 (3.98)	38.17 (7.68)	42.36 (6.46)	46.71 (9.65)	0.464	<0.001	0.045
Spine	8.16 (2.17)	11.16 (4.71)	11.04 (2.85)	14.68 (7.73)	9.69 (2.91)	13.96 (6.58)	10.97 (2.67)	16.15 (6.62)	0.018	<0.001	0.529
Shoulder	-12.07 (8.45)	-13.71 (9.17)	-5.01 (6.25)	-6.21 (7.62)	-8.74 (7.68)	-11.71 (8.52)	-1.69 (7.25)	-5.8 (7.04)	0.325	<0.001	0.444
Elbow	5 (1.82)	6.15 (2.64)	5.47 (2.12)	8.75 (4.24)	4.91 (2.15)	5.89 (1.92)	4.87 (2)	8.53 (5.58)	0.018	0.001	0.006

Note: Means and standard deviations are provided for descriptive statistics (standard deviations are presented in parentheses). Significant p-values are in bold.

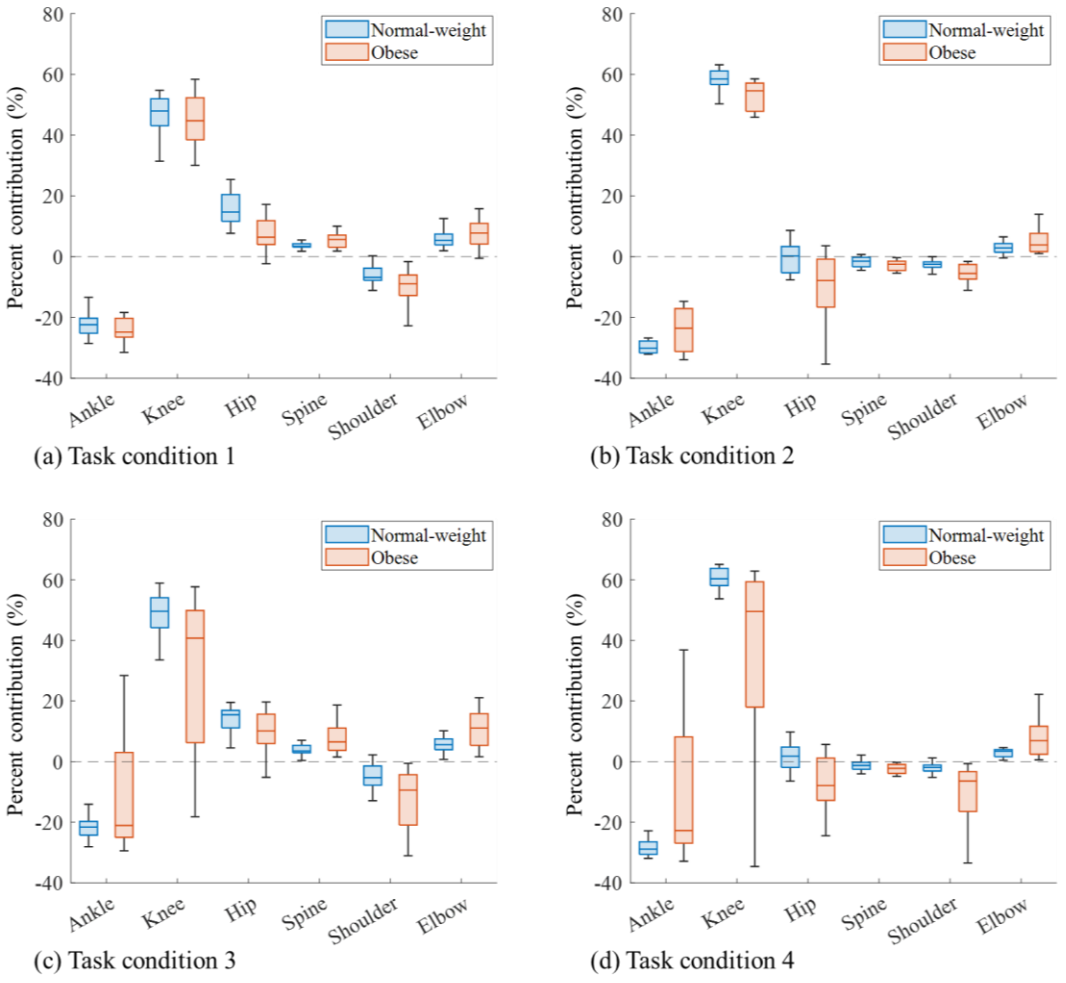

Figure 4.11: Box plots summarizing the JCV_x data for the two obesity levels in each task condition.

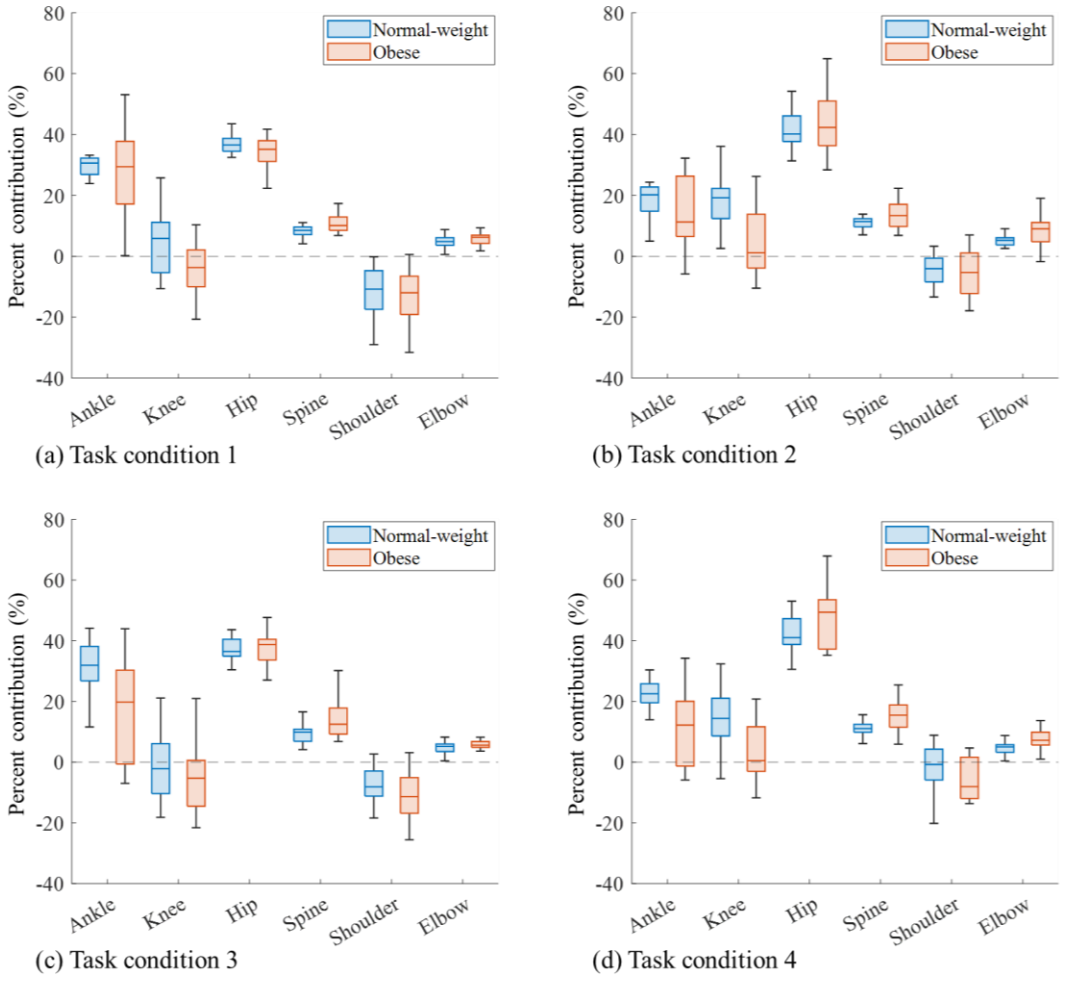

Figure 4.12: Box plots summarizing the JCV_y data for the two obesity levels in each task condition.

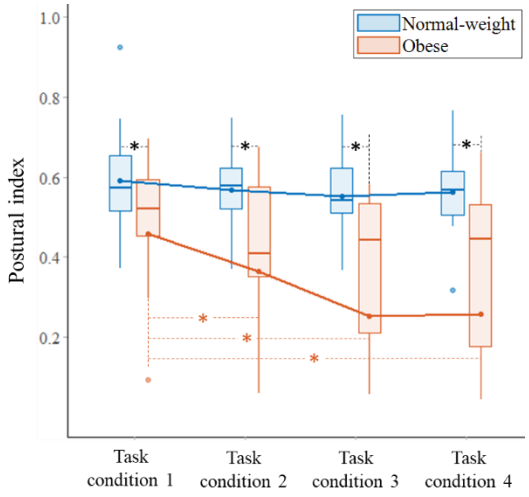

Figure 4.13: Obesity Level × Task Condition interaction effects on postural index. '*' denotes significant pairwise differences on Obesity Level or Task Condition.

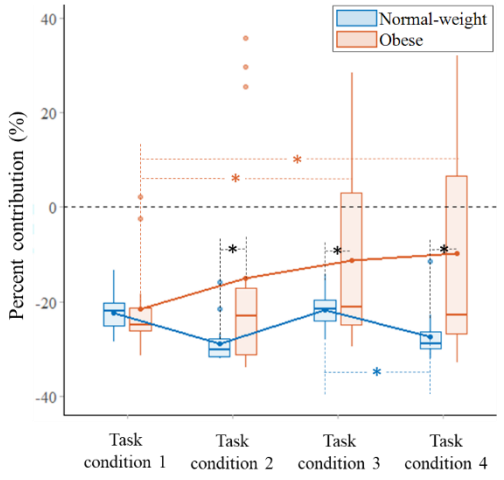

(a) PC_x of the ankle joint

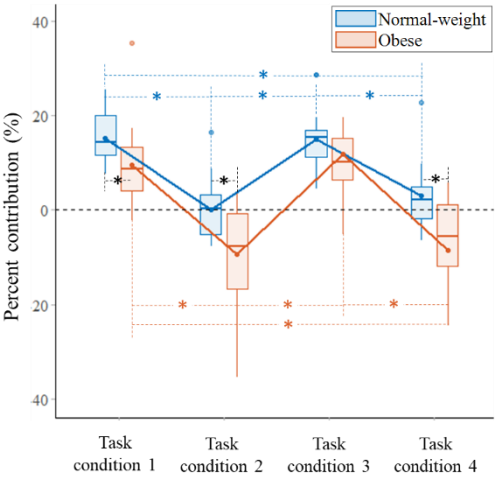

(b) PC_x of the hip joint

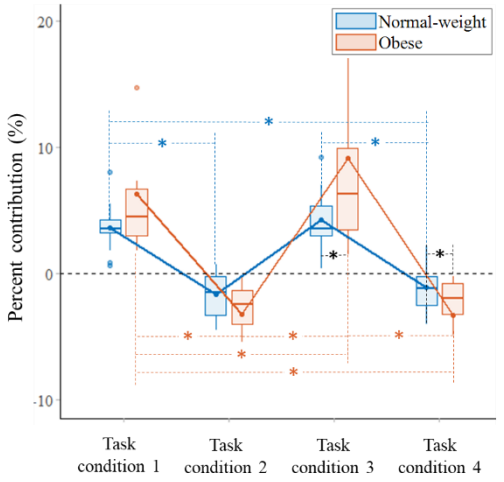

(c) PC_x of the spine joint

Figure 4.14: Obesity Level × Task Condition interaction effects on PC_x values: (a) the ankle joint, (b) the hip joint, and (c) the spine joint. '*' denotes significant pairwise differences on Obesity Level or Task Condition.

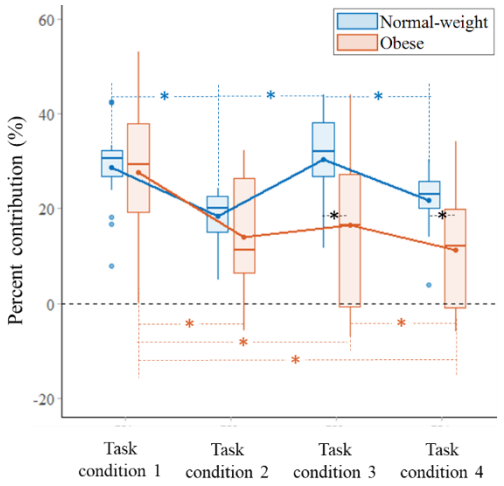

(a) PC_y of the ankle joint

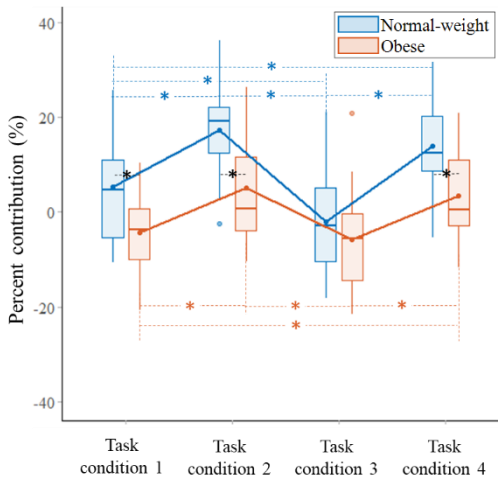

(b) PC_y of the knee joint

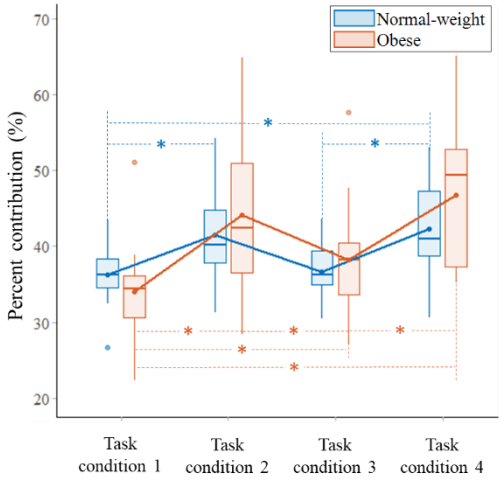

(c) PC_y of the hip joint

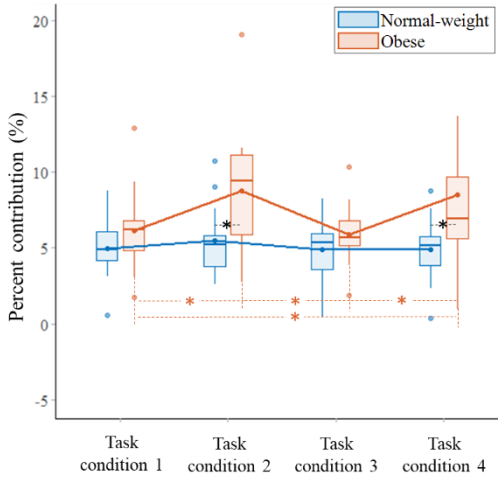

(d) PC_y of the elbow joint

Figure 4.15: Obesity Level × Task Condition interaction effects on PC_y values: (a) the ankle joint, (b) the knee joint, (c) the hip joint, and (d) the elbow joint. '*' denotes significant pairwise differences on Obesity Level or Task Condition.

4.4 Discussion

This study investigated the impacts of severe obesity on the joint kinematics and movement technique during sagittally symmetric manual lifting under four task conditions. Obese and normal-weight participants performed manual lifting with box weights equal to the RWLs, and the lifting movements were recorded by a motion capture system. The obese and normal-weight groups were compared in a set of kinematics variables and movement technique indexes.

Some major study findings were as follows:

<Obesity Level impacts on kinematic variables>

- The obese group showed a larger mean task duration than the normal-weight group (Table 4.3 and Figure 4.6).

- Mean ROE was smaller for the obese group than the normal-weight group for the ankle, knee, hip and elbow joints (Table 4.4 and Figure 4.7).

- The obese group showed a smaller mean absolute joint angular velocity than the normal-weight group at all but the spine joint (Table 4.5 and Figure 4.8).

- The obese group showed a smaller peak angular acceleration than the normal-weight group for the knee and elbow joints (Table 4.6 and Figure 4.9).

<Obesity Level impacts on movement technique indexes>

- The obese group had a smaller mean postural index value than the normal-weight group (Table 4.7).

- For JCV_x, mean absolute PC values for the ankle and knee joints were smaller for the obese group than the normal-weight group; on the other hand, mean absolute PC values for the shoulder and elbow joints were larger for the obese group than the normal-weight group (Table 4.8 and Figure 4.11).

- For JCV_y, mean absolute PC values for the ankle and knee joints were smaller for the obese group than the normal-weight group; on the other hand, mean absolute PC values for the spine and elbow joints were larger for the obese group than the normal-weight group (Table 4.9 and Figure 4.12).

<Task Condition effects & interaction effects>

- Task Condition was found to be significant for many of the dependent variables (Table 4.3-4.9, Figure 4.6-4.9, and Figures 4.11-4.12).

- Some significant Obesity Level × Task Condition interaction effects were found (Table 4.3-4.9, Figure 4.10, and Figures 4.13-4.15).

The relatively slow lifting movements in the obese group (Table 4.3, Tables 4.5 and 4.6, Figure 4.6, and Figures 4.8 and 4.9) could be attributed to difficulties in

shifting the body center of mass (COM) into the base of support (BOS) to maintain postural balance. Obesity is associated with increased postural sway amplitude [70], [112], [113], and the increased postural sway could reduce the postural stability by reducing the distance between the boundary of the BOS and the COM [114]. In addition, obese participants were expected to require the larger ankle plantar flexion moment to avoid loss of stability under postural perturbation [115].

Moreover, the inverted pendulum model with foot segment [116] could simulate the feasible region of the body COM to maintain the balance under physical constraints such as ankle strength, foot geometry, and contact force. Maktouf et al. [117] showed that the maximum voluntary force in ankle dorsal/plantar flexion was not significantly different between the obese and normal-weight groups. For the inverted pendulum model [116] with the ankle strength condition [117], it could be expected that the feasible region of the COM of the obese participant would be narrower than that of the normal-weight participant. Therefore, the slower movements of the obese participants could be a lifting technique to compensate for the reduction of stability. Also, it has been consistently observed that the obese participants performed the tasks slowly in manual material handling [118] and seated foot reaches [37].

The muscle force-velocity relationship might be associated with the slower movements in the obese participants. The contraction of the muscle is driven by the sliding of actin and myosin filaments [119], and the force generated by the muscle

depends on the number of actin and myosin cross-bridges [120]. As the actin and myosin slide over each other slowly, both the muscle's ability to form cross-bridges and the muscle force-generating capacity increase [120]. Since the obese participant with heavier body mass required greater muscle forces to lift a box, they might select slower lifting movements, which are advantageous in terms of muscle force generation.

The slow movements of the obese group might also be associated with slowed information processing and motor control due to obesity-related cognitive dysfunction. Several experimental studies support that obesity is associated with deterioration of gross motor skill performance such as upper-limb coordination and difficulty with perceptual-motor coordination [121]–[123]. Additionally, functional magnetic resonance imaging (fMRI) studies were used to investigate the effects of obesity on white matter dysfunction in the brain [124], [125]. The disruption of white matter is associated with a decrease in neural transmission speed and slow information processing [124], [125], which is characterized by the less anisotropic orientation of the nerve fiber bundles measured by fMRI [125], [126]. Several studies found a negative correlation between BMI and the anisotropy in the white matter [123]–[125], and, therefore, obesity is associated with impairment of neurocognitive function, suggesting that it has the potential to interfere with sensory integration for motor control, resulting in the slow movements.

Compared to the normal-weight participants, the obese participants showed

smaller ROEs at the joints other than the spine joints (Table 4.4 and Figure 4.7), which could be explained in terms of muscle strength and mechanical work. The absolute strength of weight-bearing muscles (e.g., quadriceps and trunk muscles) of the obese group generally exceeds that of the normal-weight group [34], [103], [127], [128]. However, the relative strength (%body mass) of the weight-bearing muscles was lower in the obese participant than in the normal-weight participant [36], [129]. Excursion angles of the joints are associated with external mechanical work in body segment motions. As the obese participants had heavier body segments [130]–[132] and lower relative muscle strengths [36], [129] than the normal-weight participants, it appears that lifting with smaller joint ROEs were likely chosen for the obese participants to reduce the mechanical work done in lifting movements.

The peak angular acceleration of the obese group, which is significantly lower than that of the normal-weight group (Table 4.6 and Figure 4.9), could be explained by simple physics considering the increase of body mass. Acceleration of body segments during the dynamic task increases the loads on the musculoskeletal system [77], [133], [134] such as the joint force, and the load caused by the acceleration constitutes a significant proportion of the net load in the dynamic task [133], [134]. For obese participants, the load increased by the acceleration could be further adversely affected by their excess body mass (F=ma), and, therefore, it is possible that the obese participant consciously or unconsciously adopted the movement technique that reduces the peak angular acceleration.

Moreover, obesity has been associated with increases in the moment of inertia of body segments [130], [131] and reduction of the relative muscle strength, such as knee extensor strength normalized to body weight [34], [36]. These obesity-related physiological changes might have contributed to the decrease in the angular acceleration of the knee joint in obese participants ($\tau=I\alpha$), and, thus, could result in decelerated lifting movement.

In contrast to the other joints, Obesity Level did not have a significant effect on the spine kinematics (Tables 4.4-4.6 and Figures 4.7-4.9). Previous studies also have shown that the spine movements were not affected by box load [135] and movement technique [136] during manual lifting, as well as obesity [137] during trunk forward flexion. The studies identified that a greater trunk inclination induces an increase in anterior pelvic tilt and hip flexion while maintaining lumbar flexion [135], [137]. The degree of lumbar flexion is related to the L5/S1 moment and the risk of MSDs such as low back pain [135], [137]. These suggest that Obesity Level might not exacerbate the risk of spine injury caused by increased lumbar flexion.

The obese participants adopted a lifting technique close to the stoop that extends the knee and hip at the onset of a lift (Table 4.7 and Figure 4.13). This appears to be due to mechanical obstruction caused by excessive fat and loss of stability when the obese participant tried to take the squat technique. Obesity reduces the range of motion (ROM) for knee flexion due to interposition of inter-segment [31], and the obese

participant experienced mechanical obstruction during trunk forward flexion as the abdomen contacts the anterior thigh [72]. If the obese participant grasps the box with sufficient knee flexion, the mechanical obstruction due to the abdomen-thigh contact makes the hip and spine flexion difficult. As the obese participant attempts the full squat with knee flexion, the COM deviated from the BOS in the posterior direction, resulting in a fall on the buttocks. Consequently, the obese participants had difficulty taking a full squat due to the limited ROM and postural instability, so it is more likely they would adopt the stoop at the onset of a lift.

The JCV indexes characterized the lifting movements of the normal-weight and obese participants through the contributions of individual joints to the box trajectories. The JCV_x values identified that the ankle and knee joints were major contributors to the box trajectory for both participant groups (Table 4.8 and Figure 4.11). Also, the JCV_y values revealed that the lifting motions of the two participant groups primarily rely on the ankle and hip joints (Table 4.9 and Figure 4.12).

The obese group had lower contributions of the ankle and knee joints in horizontal (JCV_x) and vertical directions (JCV_y) compared to the normal-weight group. The elbow joint, however, showed a greater contribution in both horizontal and vertical directions (Tables 4.8-4.9 and Figures 4.11-4.12). The relative mass (%total body mass) of the hands and forearms of obese participants was smaller than that of normal-weight participants, but the total relative mass of the trunk, neck, and head

was greater [132]. Therefore, the obese participants might show an efficient movement technique in terms of energy expenditure by reducing the contribution of the joints supporting heavy upper segments, and increasing the contribution of the joints associated with the relatively light segments.

The results showed that significant interaction effects between Obesity Level and Task Condition on postural index (Table 4.7 and Figure 4.13). The normal-weight group showed no significant difference in postural index by Task Condition, but the obese group showed a decrease in postural index in Task Condition where the horizontal location of the destination increased. In other words, recognizing the task goal influenced the selection of motor planning that determines the initial lifting posture of the obese participants. The lifting technique close to stoop has the following advantages: 1) more efficient than squat in terms of energy expenditure and ventilation [138]–[140], 2) lower quadriceps activation [141], [142], 3) less mechanical obstruction and reduced need for flexibility [31], and 4) reduction of the net moment of the hip joint due to abdomen-thigh contact [72]. Biomechanical studies indicate that with increasing horizontal distance of the load from the ankle, the loads such as L5/S1 compression force and hip moment increase [77], [143]. Therefore, the selection of the stoop technique in horizontally distant lifting might be associated with the alleviation of the loads on the obese participants.

The interaction effects between Obesity Level and Task Condition on the ROE

and mean absolute angular velocity were shown in Figure 4.10. When the horizontal location of the destination increased, the obese group took the lifting technique close to the stoop (Figure 4.13), which made the ankle and knee joint angles of the obese participants closer to 0 degrees. This posture left little room for changes in the angle of the ankle and knee joints during load lifting. Reduced ROEs due to the stoop technique might result in the ROE of the ankle joint and angular velocities of the ankle and knee joints being less sensitive to Task Condition.

The study findings would provide useful knowledge for the ergonomic design of the work system that accommodates obese individuals. The following design implications could be suggested on the basis of the current study findings. First, workplace layout should take into account obesity-related characteristics, such as the mechanical obstruction in forward reaching, so that obese workers could adopt the stoop lifting technique. Obese workers could be at risk of losing stability or falling if they are forced to use the squat technique during manual lifting. Second, the work system design would also consider the slow movements of obese people. In a manufacturing process such as an assembly line, it is imperative that obese workers are given sufficient time to process a work unit (e.g., standard time). Third, the results of this study could be utilized to design wearable equipment such as personal lift assist devices and military exoskeletons. Existing personal lift assist devices were mainly designed to assist the spine and hip joints [144]–[149]. In the light of the high contribution of the knee joint during manual lifting (Tables 4.8-4.9 and Figures 4.11-

4.12), a design that includes a function to assist the knee needs to be considered.

Some limitations of the current study are described, and future research ideas are provided. First, it is acknowledged that the current study did not examine the asymmetric task conditions, which are considered as a risk factor of WMSDs in the manual lifting task [77]. Motions such as axial trunk rotation in asymmetric tasks increase the stress on the passive connective tissues of the lumbar spine [14], [79]. Thus, future studies are needed to investigate the impacts of obesity on lifting movements in asymmetric task conditions. Second, future studies may need to examine the impact of body shape type on joint kinematics and lifting techniques in obese individuals. Obese individuals could be characterized into two types according to the distribution of adipose tissue; android and gynoid somatotypes, involving central/abdominal and peripheral fat distributions, respectively [150], [151]. The accumulation of adiposity tissue could be related to the mechanical obstruction between inter-segments, which would help to explain the large within-group variability in postural index of the obese group. Third, the BMI was utilized as an indicator of overall adiposity in the current study. Since the BMI is not an index that is directly related to body composition, participants could have high fat-free mass or high fat mass even if they have identical BMIs; yet, it would be difficult to find cases with low fat mass in severely obese participants. In a future study, it would be necessary to define the participant groups based on measures such as a fat-free mass index [152] to investigate the impacts of excessive fat mass on the movement techniques.

Chapter 5

Conclusion

5.3 Summary

Working in stressful postures and movements increases the risk of work-related musculoskeletal disorders (WMSDs). The physical stress on a worker's musculoskeletal system depends on the type of work task. In the case of sedentary work, stressful sitting postures for prolonged durations could increase the load on soft connective tissues such as muscles and ligaments, resulting in the incidence of WMSDs. Therefore, to reduce the WMSDs, it is necessary to monitor a worker's sitting posture and additionally provide ergonomic interventions. When the worker performs a task that involves dynamic movements, such as manual lifting, the worker's own body mass affects the physical stress of the manual task. In the global prevalence of obesity in the workforce, an increase in the body weight of the workers could adversely affect the musculoskeletal system during the manual lifting task. Therefore, obesity could be associated with the development of WMSDs, and the impacts of obesity on workers' movement during manual lifting need to be examined.

Therefore, the purpose of this study was to: 1) develop a sensor-embedded posture classification system that is capable of classifying an instantaneous sitting

posture as one of the posture categories discussed in the ergonomics literature while not suffering from the limitations of the previous system, and, 2) identify the impacts of severe obesity on joint kinematics and movement technique during manual lifting under various task conditions. To accomplish the research objectives, two major studies were conducted.

In the study on the posture classification system, a novel sensor-embedded smart chair system was developed to monitor and classify a worker's sitting postures in real time. The smart chair system was a mixed sensor system utilizing six pressure sensors and six infrared reflective distance sensors in combination. The pressure sensors were embedded in the seat cushion to gather seat cushion pressure distribution data. The distance sensors were placed in the seatback to measure seatback-trunk distances at different locations in the frontal plane. The use of the seatback distance sensors represented a unique design feature, which distinguished the mixed sensor system from the previous posture monitoring systems. Employing a k-Nearest Neighbor algorithm, the mixed sensor system classified an instantaneous posture as one of posture categories determined based on an analysis of the ergonomics literature on sitting postures and sitting-related musculoskeletal problems. The mixed sensor system was evaluated in posture classification performance in comparison with two benchmark systems that utilized only a single type of sensors. The purpose of the comparisons was to determine the utility of the design combining seat cushion pressure sensors and seatback distance sensors. The mixed sensor system yielded significantly superior classification

performance than the two benchmark systems. The mixed sensor system is low-cost utilizing only a small number of sensors; yet, it accomplishes accurate classification of postures relevant to the ergonomic analyses of seated work tasks. The mixed sensor system could be utilized for various applications including the development of a real-time posture feedback system for preventing sitting-related musculoskeletal disorders.

In the study on the manual lifting task, optical motion capture was conducted to examine differences in joint kinematics and movement technique between severely obese and non-obese groups. A total of thirty-five subjects without a history of WMSDs participated in the experiment. The kinematic variables based on joint angles were obtained to represent the movement of individual joints. The two indexes including postural index and joint contribution vectors were utilized to characterize the lifting movement techniques. Two participant groups were statistically compared in kinematic variables and movement technique indexes. The severely obese and non-obese groups show significant differences in most joint kinematics of the ankle, knee, hip, spine, shoulder, and elbow. There were also significant differences between the groups in the movement technique index, which represents a motion in terms of the relative contribution of an individual joint degree of freedom to the box trajectory in a manual lifting task. Overall, the severely obese group adopted the back lifting technique (stoop) rather than the leg lifting technique (squat), and showed less joint range of excursion and slow movements compared to the non-obese group.

5.4 Implications

The mixed sensor system presented in this study may have various applications. The mixed sensor system could be combined with a real-time feedback/warning system to help the users adjust their postures and thereby contribute to reducing the risk of WMSDs. Another possible application of the mixed sensor system currently under our consideration is estimating the seated worker's mental workload from conducting a cognitive task on the basis of real-time posture measurements. Such mental workload estimation could serve as a basis for optimizing job scheduling.

The findings in the manual lifting study would provide useful knowledge for the ergonomic design of the work system that accommodates obese individuals. The following design implications could be suggested on the basis of the current study findings. First, workplace layout should take into account obesity-related characteristics, such as the mechanical obstruction in forward reaching, so that obese workers could adopt the stoop lifting technique. Obese workers could be at risk of losing stability or falling if they are forced to use the squat technique during manual lifting. Second, the work system design would also consider the slow movements of obese people. In a manufacturing process such as an assembly line, it is imperative that obese workers are given sufficient time to process a work unit (e.g., standard time). Third, the results of this study could be utilized to design wearable equipment such as personal lift assist devices and military exoskeletons. Existing personal lift assist devices were mainly

designed to assist the spine and hip joints [144]–[149]. In the light of the high contribution of the knee joint during manual lifting (Tables 4.8-4.9 and Figures 4.11-4.12), a design that includes a function to assist the knee needs to be considered.

5.5 Limitations and Future Works

Some limitations of the current study are described here along with future research ideas. In the study on the posture classification system, further research may be conducted to improve the current mixed sensor system. It is expected that posture classification accuracy is affected by the locations of the pressure and distance sensors [50]. By exploring different sensor placement possibilities, it may be possible to identify new designs that achieve equivalent or enhanced performance with a smaller number of sensors. Also, a future study is warranted to compare the mixed sensor system of the current study against smart chair systems that employ the same number of sensors of a single type, that is, a pressure sensors only system with 12 pressure sensors and a distance sensors only system with 12 distance sensors. Such a study may provide additional information regarding the benefits of combining different types of sensors.

In the study on the manual lifting, some limitations and future research ideas are provided. First, it is acknowledged that the current study did not examine the asymmetric task conditions, which are considered as a risk factor of WMSDs in the manual lifting task [77]. Motions such as axial trunk rotation in asymmetric tasks

increase the stress on the passive connective tissues of the lumbar spine [14], [79]. Thus, future studies are needed to investigate the impacts of obesity on lifting movements in asymmetric task conditions. Second, future studies may need to examine the impact of body shape type on joint kinematics and lifting techniques in obese individuals. Obese individuals could be characterized into two types according to the distribution of adipose tissue; android and gynoid somatotypes, involving central/abdominal and peripheral fat distributions, respectively [150], [151]. The accumulation of adiposity tissue could be related to the mechanical obstruction between inter-segments, which would help to explain the large within-group variability in postural index of the obese group. Third, the BMI was utilized as an indicator of overall adiposity in the current study. Since the BMI is not an index that is directly related to body composition, participants could have high fat-free mass or high fat mass even if they have identical BMIs; yet, it would be difficult to find cases with low fat mass in severely obese participants. In a future study, it would be necessary to define the participant groups based on measures such as a fat-free mass index [152] to investigate the impacts of excessive fat mass on the movement techniques.

Bibliography

[1] A. M. Genaidy, A. A. Al-Shedi, and W. Karwowski, "Postural stress analysis in industry," *Appl. Ergon.*, vol. 25, no. 2, pp. 77–87, 1994, doi: 10.1016/0003-6870(94)90068-X.

[2] M. H. Liao and C. G. Drury, "Posture, discomfort and performance in a vdt task," *Ergonomics*, vol. 43, no. 3, pp. 345–359, 2000, doi: 10.1080/001401300184459.

[3] E. Grandjean and W. Hünting, "Ergonomics of posture-Review of various problems of standing and sitting posture," *Appl. Ergon.*, vol. 8, no. 3, pp. 135–140, 1977, doi: 10.1016/0003-6870(77)90002-3.

[4] J. Faucett and D. Rempel, "VDT-related musculoskeletal symptoms: Interactions between work posture and psychosocial work factors," *Am. J. Ind. Med.*, vol. 26, no. 5, pp. 597–612, Nov. 1994, doi: 10.1002/ajim.4700260503.

[5] L. Ortiz-Hernández, S. Tamez-González, S. Martínez-Alcántara, and I. Méndez-Ramírez, "Computer use increases the risk of musculoskeletal disorders among newspaper office workers," *Arch. Med. Res.*, vol. 34, no. 4, pp. 331–342, 2003, doi: 10.1016/S0188-4409(03)00053-5.

[6] S. M. Van Niekerk, Q. Louw, C. Vaughan, K. Grimmer-Somers, and K. Schreve, "Photographic measurement of upper-body sitting posture of high school students: A reliability and validity study," *BMC Musculoskelet. Disord.*,

vol. 9, pp. 1–11, 2008, doi: 10.1186/1471-2474-9-113.

[7] G. Healy *et al.*, "Reducing prolonged sitting in the workplace - An evidence review: Full report," Melbourne, Australia, 2012.

[8] J. Dul and V. H. Hildebrandt, "Ergonomie guidelines for the prevention of low back pain at the workplace," *Ergonomics*, vol. 30, no. 2, pp. 419–429, 1987, doi: 10.1080/00140138708969728.

[9] N. J. Delleman and J. Dul, "International standards on working postures and movements ISO 11226 and EN 1005-4," *Ergonomics*, vol. 50, no. 11, pp. 1809–1819, 2007, doi: 10.1080/00140130701674430.

[10] S. I. S. Enanv, H. Medical, S. Ab, and S. Bertling, "Ergonomics-Evaluation of Static Working Postures," ISO 11225:2000(E), 2010.

[11] M. Vergara and Á. Page, "Relationship between comfort and back posture and mobility in sitting-posture," *Appl. Ergon.*, vol. 33, no. 1, pp. 1–8, 2002, doi: 10.1016/S0003-6870(01)00056-4.

[12] S. Gallagher, "Physical limitations and musculoskeletal complaints associated with work in unusual or restricted postures: A literature review," *J. Safety Res.*, vol. 36, no. 1, pp. 51–61, 2005, doi: 10.1016/j.jsr.2004.12.001.

[13] D. Kee and W. Karwowski, "LUBA: An assessment technique for postural loading on the upper body based on joint motion discomfort and maximum holding time," *Appl. Ergon.*, vol. 32, no. 4, pp. 357–366, 2001, doi: 10.1016/S0003-6870(01)00006-0.

[14] A. Torén, "Muscle activity and range of motion during active trunk rotation in a sitting posture," *Appl. Ergon.*, vol. 32, no. 6, pp. 583–591, 2001, doi: 10.1016/S0003-6870(01)00040-0.

[15] A. Naddeo, N. Cappetti, and C. D'Oria, "Proposal of a new quantitative method for postural comfort evaluation," *Int. J. Ind. Ergon.*, vol. 48, pp. 25–35, Jul. 2015, doi: 10.1016/j.ergon.2015.03.008.

[16] Ç. Tüzün, İ. İ. Yorulmaz, A. Cindaş, and S. Vatan, "Low Back Pain and Posture," *Clin. Rheumatol.*, vol. 18, no. 4, pp. 308–312, Jun. 1999, doi: 10.1007/s100670050107.

[17] A. Bodén and K. Öberg, "Torque resistance of the passive tissues of the trunk at axial rotation," *Appl. Ergon.*, vol. 29, no. 2, pp. 111–118, 1998, doi: 10.1016/S0003-6870(97)00030-6.

[18] O. Huxhold, S. C. Li, F. Schmiedek, and U. Lindenberger, "Dual-tasking postural control: Aging and the effects of cognitive demand in conjunction with focus of attention," *Brain Res. Bull.*, vol. 69, no. 3, pp. 294–305, 2006, doi: 10.1016/j.brainresbull.2006.01.002.

[19] K. Z. H. Li and U. Lindenberger, "Relations between aging sensory/sensorimotor and cognitive functions," *Neurosci. Biobehav. Rev.*, vol. 26, no. 7, pp. 777–783, 2002, doi: 10.1016/S0149-7634(02)00073-8.

[20] I. Olivier, R. Cuisinier, M. Vaugoyeau, V. Nougier, and C. Assaiante, "Dual-task study of cognitive and postural interference in 7-year-olds and adults,"

Neuroreport, vol. 18, no. 8, pp. 817–821, 2007, doi: 10.1097/WNR.0b013e3280e129e1.

[21] "Obesity and overweight." [Online]. Available: https://www.who.int/news-room/fact-sheets/detail/obesity-and-overweight. [Accessed: 02-Dec-2021].

[22] S. Meeuwsen, G. W. Horgan, and M. Elia, "The relationship between BMI and percent body fat, measured by bioelectrical impedance, in a large adult sample is curvilinear and influenced by age and sex," *Clin. Nutr.*, vol. 29, no. 5, pp. 560–566, Oct. 2010, doi: 10.1016/j.clnu.2009.12.011.

[23] E. Ehrampoush *et al.*, "New anthropometric indices or old ones: Which is the better predictor of body fat?," *Diabetes Metab. Syndr. Clin. Res. Rev.*, vol. 11, no. 4, pp. 257–263, Oct. 2017, doi: 10.1016/j.dsx.2016.08.027.

[24] "Obesity: Definition, Causes, Diagnosis, Treatment & More." [Online]. Available: https://www.healthline.com/health/obesity. [Accessed: 02-Dec-2021].

[25] "WHO/Europe | Nutrition - Body mass index - BMI." [Online]. Available: https://www.euro.who.int/en/health-topics/disease-prevention/nutrition/a-healthy-lifestyle/body-mass-index-bmi. [Accessed: 02-Dec-2021].

[26] M. Di Cesare *et al.*, "Trends in adult body-mass index in 200 countries from 1975 to 2014: a pooled analysis of 1698 population-based measurement studies with 19·2 million participants," *Lancet*, vol. 387, no. 10026, pp. 1377–1396, Apr. 2016, doi: 10.1016/S0140-6736(16)30054-X.

[27] C. M. Hales, C. D. Fryar, M. D. Carroll, D. S. Freedman, and C. L. Ogden, "Trendsinobesity and severe obesity prevalence in usyouth and adultsby sex and age, 2007-2008 to 2015-2016," *JAMA - J. Am. Med. Assoc.*, vol. 319, no. 16, pp. 1723–1725, Apr. 2018, doi: 10.1001/jama.2018.3060.

[28] A. J. Caban, D. J. Lee, L. E. Fleming, O. Gómez-Márin, W. LeBlanc, and T. Pitman, "Obesity in US workers: The National Health Interview Survey, 1986 to 2002," *Am. J. Public Health*, vol. 95, no. 9, pp. 1614–1622, Sep. 2005, doi: 10.2105/AJPH.2004.050112.

[29] N. P. Pronk, "Fitness of the US Workforce," *http://dx.doi.org/10.1146/annurev-publhealth-031914-122714*, vol. 36, pp. 131–149, Mar. 2015, doi: 10.1146/ANNUREV-PUBLHEALTH-031914-122714.

[30] P. Capodaglio, G. Castelnuovo, A. Brunani, L. Vismara, V. Villa, and E. Maria Capodaglio, "Functional limitations and occupational issues in obesity: A review," *Int. J. Occup. Saf. Ergon.*, vol. 16, no. 4, pp. 507–523, 2010, doi: 10.1080/10803548.2010.11076863.

[31] W. Park, J. Ramachandran, P. Weisman, and E. S. Jung, "Obesity effect on male active joint range of motion," *http://dx.doi.org/10.1080/00140130903311617*, vol. 53, no. 1, pp. 102–108, Jan. 2010, doi: 10.1080/00140130903311617.

[32] Y. Jeong, S. Heo, G. Lee, and W. Park, "Pre-obesity and obesity impacts on passive joint range of motion," *Ergonomics*, vol. 61, no. 9, pp. 1223–1231, Sep.

2018, doi: 10.1080/00140139.2018.1478455.

[33] W. Gilleard and T. Smith, "Effect of obesity on posture and hip joint moments during a standing task, and trunk forward flexion motion," *Int. J. Obes. 2007 312*, vol. 31, no. 2, pp. 267–271, Jun. 2006, doi: 10.1038/sj.ijo.0803430.

[34] N. A. Maffiuletti *et al.*, "Differences in quadriceps muscle strength and fatigue between lean and obese subjects," *Eur. J. Appl. Physiol.*, vol. 101, no. 1, pp. 51–59, 2007, doi: 10.1007/s00421-007-0471-2.

[35] C. L. Lafortuna, N. A. Maffiuletti, F. Agosti, and A. Sartorio, "Gender variations of body composition, muscle strength and power output in morbid obesity," *Int. J. Obes. 2005 297*, vol. 29, no. 7, pp. 833–841, Apr. 2005, doi: 10.1038/sj.ijo.0802955.

[36] N. Miyatake *et al.*, "Clinical evaluation of muscle strength in 20–79-years-old obese Japanese," *Diabetes Res. Clin. Pract.*, vol. 48, no. 1, pp. 15–21, Apr. 2000, doi: 10.1016/S0168-8227(99)00132-1.

[37] S. Baek, J. Jung, P. Moon, and W. Park, "Obesity impacts on task performance and perceived discomfort during seated foot target reaches," *Ergonomics*, 2021, doi: 10.1080/00140139.2021.1933202.

[38] A. Goettler, A. Grosse, and D. Sonntag, "Productivity loss due to overweight and obesity: a systematic review of indirect costs," *BMJ Open*, vol. 7, no. 10, p. e014632, Oct. 2017, doi: 10.1136/BMJOPEN-2016-014632.

[39] H. W. Rodbard, K. M. Fox, and S. Grandy, "Impact of obesity on work productivity and role disability in individuals with and at risk for diabetes mellitus," *Am. J. Heal. Promot.*, vol. 23, no. 5, pp. 353–360, May 2009, doi: 10.4278/ajhp.081010-QUAN-243.

[40] J. T. Howard and L. B. Potter, "An assessment of the relationships between overweight, obesity, related chronic health conditions and worker absenteeism," *Obes. Res. Clin. Pract.*, vol. 8, no. 1, pp. e1–e15, Jan. 2014, doi: 10.1016/J.ORCP.2012.09.002.

[41] S. Arteaga *et al.*, "Low-cost accelerometry-based posture monitoring system for stroke survivors," in *10th international ACM SIGACCESS conference on Computers and accessibility*, 2008, pp. 243–244, doi: 10.1145/1414471.1414519.

[42] L. E. Dunne, P. Walsh, S. Hermann, B. Smyth, and B. Caulfield, "Wearable monitoring of seated spinal posture," *IEEE Trans. Biomed. Circuits Syst.*, vol. 2, no. 2, pp. 97–105, 2008, doi: 10.1109/TBCAS.2008.927246.

[43] F. Abyarjoo *et al.*, "PostureMonitor: Real-Time IMU Wearable Technology to Foster Poise and Health," in *Design, User Experience, and Usability: Interactive Experience Design*, 2015, vol. 9188, pp. 543–552, doi: 10.1007/978-3-319-20889-3_60.

[44] J. Lee, E. Cho, M. Kim, Y. Yoon, and S. Choi, "PreventFHP: Detection and warning system for Forward Head Posture," *IEEE Haptics Symp. HAPTICS*, pp. 295–298, 2014, doi: 10.1109/HAPTICS.2014.6775470.

[45] A. Nayak, "Posture Monitoring and Warning System," in *National Conference on Innovations in IT and Management (NCI2TM)*, 2014, pp. 231–235.

[46] A. Manzi, F. Cavallo, and P. Dario, "A 3D human posture approach for activity recognition based on depth camera," in *Computer Vision – ECCV 2016 Workshops*, 2016, vol. 9914, pp. 432–447.

[47] S. Mota and R. W. Picard, "Automated Posture Analysis for Detecting Learner's Interest Level," 2003, vol. 5, pp. 49–49, doi: 10.1109/CVPRW.2003.10047.

[48] J. Meyer, B. Arnrich, J. Schumm, and G. Troster, "Design and modeling of a textile pressure sensor for sitting posture classification," *IEEE Sens. J.*, vol. 10, no. 8, pp. 1391–1398, 2010, doi: 10.1109/JSEN.2009.2037330.

[49] C. Ma, W. Li, R. Gravina, and G. Fortino, "Posture Detection Based on Smart Cushion for Wheelchair Users," *Sensors*, vol. 17, no. 4, p. 719, Mar. 2017, doi: 10.3390/s17040719.

[50] B. Mutlu, A. Krause, J. Forlizzi, C. Guestrin, and J. Hodgins, "Robust, low-cost, non-intrusive sensing and recognition of seated postures," in *the 20th annual ACM symposium on User interface software and technology*, 2007, pp. 149–158, doi: 10.1145/1294211.1294237.

[51] K. Kamiya, M. Kudo, H. Nonaka, and J. Toyama, "Sitting posture analysis by pressure sensors," in *19th International Conference on Pattern Recognition (ICPR 2008)*, 2008, pp. 1–4, doi: 10.1109/icpr.2008.4761863.

[52] L. Martins *et al.*, "Intelligent Chair Sensor," in *14th International Conference on Engineering Applications of Neural Networks (EANN)*, 2013, vol. 383, no. 1, pp. 182–191, doi: 10.1007/978-3-642-41013-0_19.

[53] W. Xu, M. C. Huang, N. Amini, L. He, and M. Sarrafzadeh, "ECushion: A textile pressure sensor array design and calibration for sitting posture analysis," *IEEE Sens. J.*, vol. 13, no. 10, pp. 3926–3934, 2013, doi: 10.1109/JSEN.2013.2259589.

[54] T. Fu, "Intellichair: a Non-Intrusive Sitting Posture and Sitting Activity Recognition System," Abertay University, 2015.

[55] S. Scena and R. Steindler, "Methods for sitting posture evaluation: Static posture and applications," *Strain*, vol. 44, no. 6, pp. 423–428, 2008, doi: 10.1111/j.1475-1305.2007.00334.x.

[56] A. A. N. Shirehjini, A. Yassine, and S. Shirmohammadi, "Design and implementation of a system for body posture recognition," *Multimed. Tools Appl.*, vol. 70, no. 3, pp. 1637–1650, 2014, doi: 10.1007/s11042-012-1137-6.

[57] S. Suzuki, M. Kudo, and A. Nakamura, "Sitting posture diagnosis using a pressure sensor mat," in *ISBA 2016 - IEEE International Conference on Identity, Security and Behavior Analysis*, 2016, pp. 1–6, doi: 10.1109/ISBA.2016.7477236.

[58] G. Liang, J. Cao, and X. Liu, "Smart cushion: A practical system for fine-grained sitting posture recognition," in *2017 IEEE International Conference on*

Pervasive Computing and Communications Workshops, 2017, no. 7, pp. 419–424.

[59] B. Zhou and P. Lukowicz, "Smart blanket: a real-time user posture sensing approach for ergonomic designs," in *the AHFE 2017 International Conference on Usability and User Experience*, 2017, vol. 607, pp. 193–204, doi: 10.1007/978-3-319-60492-3.

[60] M. Kim, H. Kim, J. Park, K. K. Jee, J. A. Lim, and M. C. Park, "Real-time sitting posture correction system based on highly durable and washable electronic textile pressure sensors," *Sensors Actuators, A Phys.*, vol. 269, pp. 394–400, Jan. 2018, doi: 10.1016/j.sna.2017.11.054.

[61] J. Roh, H. Park, K. Lee, J. Hyeong, S. Kim, and B. Lee, "Sitting Posture Monitoring System Based on a Low-Cost Load Cell Using Machine Learning," *Sensors*, vol. 18, no. 208, 2018, doi: 10.3390/s18010208.

[62] M. Huang, I. Gibson, and R. Yang, "Smart Chair for Monitoring of Sitting Behavior," in *The International Conference on Design and Technology*, 2017, pp. 274–280, doi: 10.18502/keg.v2i2.626.

[63] R. Zemp *et al.*, "Application of Machine Learning Approaches for Classifying Sitting Posture Based on Force and Acceleration Sensors," *Biomed Res. Int.*, vol. 2016, 2016, doi: 10.1155/2016/5978489.

[64] D. Singh, W. Park, D. Hwang, and M. S. Levy, "Severe obesity effect on low back biomechanical stress of manual load lifting," *Work*, vol. 51, no. 2, pp.

337–348, 2015, doi: 10.3233/WOR-141945.

[65] M. Badawy *et al.*, "Trunk muscle activity among older and obese individuals during one-handed carrying," *Appl. Ergon.*, vol. 78, pp. 217–223, Jul. 2019, doi: 10.1016/J.APERGO.2019.03.007.

[66] P. Corbeil *et al.*, "Biomechanical analysis of manual material handling movement in healthy weight and obese workers," *Appl. Ergon.*, vol. 74, no. August 2018, pp. 124–133, Jan. 2019, doi: 10.1016/j.apergo.2018.08.018.

[67] X. Xu, G. A. Mirka, and S. M. Hsiang, "The effects of obesity on lifting performance," *Appl. Ergon.*, vol. 39, no. 1, pp. 93–98, 2008, doi: 10.1016/j.apergo.2007.02.001.

[68] M. Ghesmaty Sangachin and L. A. Cavuoto, "Obesity-related changes in prolonged repetitive lifting performance," *Appl. Ergon.*, vol. 56, pp. 19–26, Sep. 2016, doi: 10.1016/j.apergo.2016.03.002.

[69] A. Colim, P. Arezes, P. Flores, and A. C. Braga, "Kinematics differences between obese and non-obese workers during vertical handling tasks," *Int. J. Ind. Ergon.*, vol. 77, p. 102955, May 2020, doi: 10.1016/j.ergon.2020.102955.

[70] D. Singh, W. Park, and M. S. Levy, "Obesity does not reduce maximum acceptable weights of lift," *Appl. Ergon.*, vol. 40, no. 1, pp. 1–7, 2009, doi: 10.1016/j.apergo.2008.04.007.

[71] U. E. Larsson and E. Mattsson, "Functional limitations linked to high body mass index, age and current pain in obese women," *Int. J. Obes.*, vol. 25, no.

6, pp. 893–899, 2001, doi: 10.1038/sj.ijo.0801553.

[72] B. Singh, T. D. Brown, J. J. Callaghan, and H. J. Yack, "Abdomen-Thigh Contact During Forward Reaching Tasks in Obese Individuals," *J. Appl. Biomech.*, vol. 29, no. 5, pp. 517–524, Oct. 2013, doi: 10.1123/JAB.29.5.517.

[73] M. A. Hamilton, L. Strawderman, K. Babski-Reeves, and B. Hale, "Effects of BMI and task parameters on joint angles during simulated small parts assembly," *Int. J. Ind. Ergon.*, vol. 43, no. 5, pp. 417–424, Sep. 2013, doi: 10.1016/J.ERGON.2013.08.003.

[74] M. Pajoutan, X. Xu, and L. A. Cavuoto, "The effect of obesity on postural stability during a standardized lifting task," *http://dx.doi.org/10.1080/15459624.2016.1237032*, vol. 14, no. 3, pp. 180–186, Mar. 2017, doi: 10.1080/15459624.2016.1237032.

[75] D. Singh, W. Park, M. S. M. Levy, and E. E. S. Jung, "The effects of obesity and standing time on postural sway during prolonged quiet standing," *http://dx.doi.org/10.1080/00140130902777636*, vol. 52, no. 8, pp. 977–986, 2009, doi: 10.1080/00140130902777636.

[76] J. W. Błaszczyk, J. Cieślinska-Świder, M. Plewa, B. Zahorska-Markiewicz, and A. Markiewicz, "Effects of excessive body weight on postural control," *J. Biomech.*, vol. 42, no. 9, pp. 1295–1300, Jun. 2009, doi: 10.1016/J.JBIOMECH.2009.03.006.

[77] T. R. Waters, V. Putz-Anderson, A. Garg, and L. J. Fine, "Revised NIOSH

equation for the design and evaluation of manual lifting tasks," *Ergonomics*, vol. 36, no. 7, pp. 749–776, 1993, doi: 10.1080/00140139308967940.

[78] D. B. CHAFFIN and K. S. PARK, "A Longitudinal Study of Low-Back Pain as Associated with Occupational Weight Lifting Factors," *http://dx.doi.org/10.1080/0002889738506892*, vol. 34, no. 12, pp. 513–525, Dec. 2010, doi: 10.1080/0002889738506892.

[79] W. E. Hoogendoorn *et al.*, "Flexion and Rotation of the Trunk and Lifting at Work Are Risk Factors for Low Back Pain," *Spine (Phila. Pa. 1976).*, vol. 25, no. 23, pp. 3087–3092, 2000, doi: 10.1136/oem.58.3.200.

[80] E. K. Wai, D. M. Roffey, P. Bishop, B. K. Kwon, and S. Dagenais, "Causal assessment of occupational lifting and low back pain: results of a systematic review," *Spine J.*, vol. 10, no. 6, pp. 554–566, Jun. 2010, doi: 10.1016/J.SPINEE.2010.03.033.

[81] E. Occhipinti, D. Colombini, C. Frigo, A. Pedotti, and A. Grieco, "Sitting posture: Analysis of lumbar stresses with upper limbs supported," *Ergonomics*, vol. 28, no. 9, pp. 1333–1346, 1985, doi: 10.1080/00140138508963250.

[82] D. B. Chaffin, G. B. J. Andersson, and B. J. Martin, *Occupational Biomechanics*. 2006.

[83] J. M. Morris, G. Benner, and D. B. Lucas, "An electromyographic study of the intrinsic muscles of the back in man," *J. Anat.*, vol. 96, no. Pt 4, pp. 509–520, 1962.

[84] M. H. Pope, K. L. Goh, and M. L. Magnusson, "Spine Ergonomics," *Annu. Rev. Biomed. Eng.*, vol. 4, no. 1, pp. 49–68, 2002, doi: 10.1146/annurev.bioeng.4.092101.122107.

[85] D. S. McNally, I. M. Shackleford, A. E. Goodship, and R. C. Mulholland, "In Vivo Stress Measurement Can Predict Pain on Discography," *Spine (Phila. Pa. 1976).*, vol. 21, no. 22, pp. 2580–2587, 1996.

[86] M. Makhsous, F. Lin, J. Bankard, R. W. Hendrix, M. Hepler, and J. Press, "Biomechanical effects of sitting with adjustable ischial and lumbar support on occupational low back pain: Evaluation of sitting load and back muscle activity," *BMC Musculoskelet. Disord.*, vol. 10, no. 17, 2009, doi: 10.1186/1471-2474-10-17.

[87] B. Valachi and K. Valachi, "Preventing musculoskeletal disorders in clinical dentistry," *J. Am. Dent. Assoc.*, vol. 134, no. 12, pp. 1604–1612, 2014, doi: 10.14219/jada.archive.2003.0106.

[88] D. Treaster and W. S. Marras, "Measurement of seat pressure distributions," *Hum. Factors*, vol. 29, no. 5, pp. 563–575, 1987, doi: 10.1177/001872088702900506.

[89] J.-H. Lee, S.-Y. Park, and W.-G. Yoo, "Changes in craniocervical and trunk flexion angles and gluteal pressure during VDT work with continuous cross-legged sitting," *J. Occup. Health*, vol. 53, no. 5, pp. 350–355, 2011.

[90] H. Riihimäki, S. Tola, T. Videman, and K. Hänninen, "Low-back pain and

occupation. A cross-sectional questionnaire study of men in machine operating, dynamic physical work, and sedentary work.," *Spine (Phila. Pa. 1976).*, vol. 14, no. 2, pp. 204–209, Feb. 1989.

[91] K. A. for T. and S. KATS, "Report on the 7th Size Korea National Anthropometric Survey," 2015.

[92] L. Jiang, Z. Cai, D. Wang, and S. Jiang, "Survey of improving K-nearest-neighbor for classification," *Proc. - Fourth Int. Conf. Fuzzy Syst. Knowl. Discov. FSKD 2007*, vol. 1, pp. 679–683, 2007, doi: 10.1109/FSKD.2007.552.

[93] H. E. S. Said, T. N. Tan, and K. D. Baker, "Personal identification based on handwriting," *Pattern Recognit.*, vol. 33, no. 1, pp. 149–160, Jan. 2000, doi: 10.1016/S0031-3203(99)00006-0.

[94] E.-H. Han, G. Karypis, and V. Kumar, "Text Categorization Using Weight Adjusted k-Nearest Neighbor Classification," pp. 53–65, 2007, doi: 10.1007/3-540-45357-1_9.

[95] Y. Lei and M. J. Zuo, "Gear crack level identification based on weighted K nearest neighbor classification algorithm," *Mech. Syst. Signal Process.*, vol. 23, no. 5, pp. 1535–1547, 2009, doi: 10.1016/j.ymssp.2009.01.009.

[96] W. Cede *et al.*, "Using particle swarms for the development of QSAR models based on K-nearest neighbor and kernel regression," *J. Comput. Aided. Mol. Des.*, vol. 17, no. 2–4, pp. 255–263, Feb. 2003, doi: 10.1023/A:1025338411016.

[97] H. Liu and L. Yu, "Toward integrating feature selection algorithms for

classification and clustering," *IEEE Trans. Knowl. Data Eng.*, vol. 17, no. 4, pp. 491–502, 2005, doi: 10.1109/TKDE.2005.66.

[98] S. M. LaValle, M. S. Branicky, and S. R. Lindemann, "On the Relationship between Classical Grid Search and Probabilistic Roadmaps," *Int. J. Rob. Res.*, vol. 23, no. 7–8, pp. 673–692, Aug. 2004, doi: 10.1177/0278364904045481.

[99] J. Bergstra and Y. Bengio, "Random search for hyper-parameter optimization," *J. Mach. Learn. Res.*, vol. 13, no. 10, pp. 281–305, 2012.

[100] Y. Song, J. Huang, D. Zhou, H. Zha, and C. L. Giles, "IKNN: Informative K-Nearest Neighbor Pattern Classification," in *Knowledge Discovery in Databases: PKDD 2007*, 2007, pp. 248–264, doi: 10.1007/978-3-540-74976-9_25.

[101] D. W. Aha, *Feature Weighting for Lazy Learning Algorithms*. 1998.

[102] "Defining Adult Overweight & Obesity | Overweight & Obesity | CDC." [Online]. Available: https://www.cdc.gov/obesity/adult/defining.html. [Accessed: 28-Jan-2022].

[103] L. A. Cavuoto and M. A. Nussbaum, "Influences of Obesity on Job Demands and Worker Capacity," *Curr. Obes. Rep.*, vol. 3, no. 3, pp. 341–347, 2014, doi: 10.1007/s13679-014-0105-z.

[104] P. Buckle and J. Buckle, "Obesity, ergonomics and public health," *Perspect. Public Health*, vol. 131, no. 4, pp. 170–176, Jul. 2011, doi: 10.1177/1757913911407267.

[105] E. A. Finkelstein *et al.*, "Obesity and Severe Obesity Forecasts Through 2030," *Am. J. Prev. Med.*, vol. 42, no. 6, pp. 563–570, Jun. 2012, doi: 10.1016/J.AMEPRE.2011.10.026.

[106] M. Changulani, Y. Kalairajah, T. Peel, and R. E. Field, "The relationship between obesity and the age at which hip and knee replacement is undertaken," *J. Bone Jt. Surg. - Ser. B*, vol. 90, no. 3, pp. 360–363, Mar. 2008, doi: 10.1302/0301-620X.90B3.19782/ASSET/IMAGES/LARGE/19782-2.JPEG.

[107] H. K. Vincent, M. C. B. Adams, K. R. Vincent, and R. W. Hurley, "Musculoskeletal Pain, Fear Avoidance Behaviors, and Functional Decline in Obesity: Potential Interventions to Manage Pain and Maintain Function," *Reg. Anesth. Pain Med.*, vol. 38, no. 6, pp. 481–491, Nov. 2013, doi: 10.1097/AAP.0000000000000013.

[108] Vicon Motion Systems. *Plug-in Gait Reference Guide* (2016). Accessed: Dec. 1, 2021. [Online]. Available: https://docs.vicon.com/download/attachments/42696722/Plug-in%20Gait%20Reference%20Guide.pdf?version=1&modificationDate=1502364735000&api=v2

[109] R. Burgess-Limerick and B. Abernethy, "Toward a quantitative definition of manual lifting postures," *Hum. Factors*, vol. 39, no. 1, pp. 141–148, 1997, doi: 10.1518/001872097778940632.

[110] W. Park, B. J. Martin, S. Choe, D. B. Chaffin, and M. P. Reed, "Representing and identifying alternative movement techniques for goal-directed manual tasks," *J. Biomech.*, vol. 38, no. 3, pp. 519–527, Mar. 2005, doi: 10.1016/j.jbiomech.2004.04.014.

[111] D. C. Montgomery and J. Wiley, "Design and Analysis of Experiments Eighth Edition," 2013.

[112] F. Menegoni, M. Galli, E. Tacchini, L. Vismara, M. Cavigioli, and P. Capodaglio, "Gender-specific Effect of Obesity on Balance," *Obesity*, vol. 17, no. 10, pp. 1951–1956, Oct. 2009, doi: 10.1038/OBY.2009.82.

[113] M. Dutil *et al.*, "The impact of obesity on balance control in community-dwelling older women," *Age (Omaha).*, vol. 35, no. 3, pp. 883–890, Jun. 2013, doi: 10.1007/S11357-012-9386-X/TABLES/2.

[114] M. B. King, J. O. Judge, and L. Wolf, "Functional Base of Support Decreases With Age," *J. Gerontol. Med. Sci.*, vol. 49, no. 6, pp. 258–263, 1994.

[115] P. Corbeil, M. Simoneau, D. Rancourt, A. Tremblay, and N. Teasdale, "Increased risk for falling associated with obesity: Mathematical modeling of postural control," *IEEE Trans. Neural Syst. Rehabil. Eng.*, vol. 9, no. 2, pp. 126–136, 2001, doi: 10.1109/7333.928572.

[116] Y. C. Pai and J. Patton, "Center of mass velocity-position predictions for balance control," *J. Biomech.*, vol. 30, no. 4, pp. 347–354, Apr. 1997, doi: 10.1016/S0021-9290(96)00165-0.

[117] W. Maktouf, S. Durand, S. Boyas, C. Pouliquen, and B. Beaune, "Combined effects of aging and obesity on postural control, muscle activity and maximal voluntary force of muscles mobilizing ankle joint," *J. Biomech.*, vol. 79, pp. 198–206, 2018, doi: 10.1016/j.jbiomech.2018.08.017.

[118] P. Corbeil *et al.*, "Biomechanical analysis of manual material handling movement in healthy weight and obese workers," *Appl. Ergon.*, vol. 74, pp. 124–133, Jan. 2019, doi: 10.1016/j.apergo.2018.08.018.

[119] H. M. Holden *et al.*, "Structure of the actin-myosin complex and its implications for muscle contraction," *Science (80-.).*, vol. 261, no. 5117, pp. 58–65, 1993, doi: 10.1126/SCIENCE.8316858.

[120] D. A. Smith, *The Sliding-Filament Theory of Muscle Contraction*. Springer International Publishing, 2018.

[121] I. Gentier *et al.*, "Fine and gross motor skills differ between healthy-weight and obese children," *Res. Dev. Disabil.*, vol. 34, no. 11, pp. 4043–4051, Nov. 2013, doi: 10.1016/J.RIDD.2013.08.040.

[122] E. D'Hondt, B. Deforche, I. De Bourdeaudhuij, and M. Lenoir, "Childhood obesity affects fine motor skill performance under different postural constraints," *Neurosci. Lett.*, vol. 440, no. 1, pp. 72–75, Jul. 2008, doi: 10.1016/J.NEULET.2008.05.056.

[123] J. Liang, B. E. Matheson, W. H. Kaye, and K. N. Boutelle, "Neurocognitive correlates of obesity and obesity-related behaviors in children and adolescents,"

Int. J. Obes. 2014 384, vol. 38, no. 4, pp. 494–506, Aug. 2013, doi: 10.1038/ijo.2013.142.

[124] K. M. Stanek *et al.*, "Obesity is associated with reduced white matter integrity in otherwise healthy adults," *Obesity*, vol. 19, no. 3, pp. 500–504, 2011, doi: 10.1038/oby.2010.312.

[125] S. Kullmann, F. Schweizer, R. Veit, A. Fritsche, and H. Preissl, "Compromised white matter integrity in obesity," *Obes. Rev.*, vol. 16, no. 4, pp. 273–281, Apr. 2015, doi: 10.1111/OBR.12248/SUPPINFO.

[126] J. C. Timpe, K. C. Rowe, J. Matsui, V. A. Magnotta, and N. L. Denburg, "White matter integrity, as measured by diffusion tensor imaging, distinguishes between impaired and unimpaired older adult decision-makers: A preliminary investigation," *J. Cogn. Psychol.*, vol. 23, no. 6, pp. 760–767, 2011, doi: 10.1080/20445911.2011.578065.

[127] Y. Rolland, V. Lauwers-Cances, M. Pahor, J. Fillaux, H. Grandjean, and B. Vellas, "Muscle strength in obese elderly women: effect of recreational physical activity in a cross-sectional study," *Am. J. Clin. Nutr.*, vol. 79, no. 4, pp. 552–557, Apr. 2004, doi: 10.1093/AJCN/79.4.552.

[128] M. Hulens, G. Vansant, R. Lysens, A. L. Claessens, E. Muls, and S. Brumagne, "Study of differences in peripheral muscle strength of lean versus obese women: an allometric approach," *Int. J. Obes. 2001 255*, vol. 25, no. 5, pp. 676–681, May 2001, doi: 10.1038/sj.ijo.0801560.

[129] N. A. Maffiuletti, S. Ratel, A. Sartorio, and V. Martin, "The Impact of Obesity on In Vivo Human Skeletal Muscle Function," *Curr. Obes. Rep.*, vol. 2, no. 3, pp. 251–260, 2013, doi: 10.1007/s13679-013-0066-7.

[130] R. Pryce and D. Kriellaars, "Body segment inertial parameters and low back load in individuals with central adiposity," *J. Biomech.*, vol. 47, no. 12, pp. 3080–3086, Sep. 2014, doi: 10.1016/J.JBIOMECH.2014.06.038.

[131] S. L. Matrangola, M. L. Madigan, M. A. Nussbaum, R. Ross, and K. P. Davy, "Changes in body segment inertial parameters of obese individuals with weight loss," *J. Biomech.*, vol. 41, no. 15, pp. 3278–3281, Nov. 2008, doi: 10.1016/J.JBIOMECH.2008.08.026.

[132] R. L. Whittaker, M. E. Vidt, R. M. E. Lockley, M. Mourtzakis, and C. R. Dickerson, "Upper extremity and trunk body segment parameters are affected by BMI and sex," *J. Biomech.*, vol. 117, p. 110230, Mar. 2021, doi: 10.1016/J.JBIOMECH.2021.110230.

[133] S. A. Lavender, Y. C. Li, G. B. J. Andersson, and R. N. Natarajan, "The effects of lifting speed on the peak external forward bending, lateral bending, and twisting spine moments," *https://doi.org/10.1080/001401399185838*, vol. 42, no. 1, pp. 111–125, Jan. 2010, doi: 10.1080/001401399185838.

[134] S. M. McGill and R. W. Norman, "Dynamically and statically determined low back moments during lifting," *J. Biomech.*, vol. 18, no. 12, pp. 877–885, Jan. 1985, doi: 10.1016/0021-9290(85)90032-6.

[135] J. R. Potvin, S. M. McGill, and R. W. Norman, "Trunk muscle and lumbar ligament contributions to dynamic lifts with varying degrees of trunk flexion," *Spine (Phila. Pa. 1976).*, vol. 16, no. 9, pp. 1099–1107, 1991, doi: 10.1097/00007632-199109000-00015.

[136] K. P. Gill, S. J. Bennett, G. J. P. Savelsbergh, and J. H. Van Dieën, "Regional changes in spine posture at lift onset with changes in lift distance and lift style," *Spine (Phila. Pa. 1976).*, vol. 32, no. 15, pp. 1599–1604, Jul. 2007, doi: 10.1097/BRS.0B013E318074D492.

[137] L. Vismara, F. Menegoni, F. Zaina, M. Galli, S. Negrini, and P. Capodaglio, "Effect of obesity and low back pain on spinal mobility: A cross sectional study in women," *J. Neuroeng. Rehabil.*, vol. 7, no. 1, pp. 1–8, Jan. 2010, doi: 10.1186/1743-0003-7-3/FIGURES/5.

[138] L. Straker, "Evidence to support using squat, semi-squat and stoop techniques to lift low-lying objects," *Int. J. Ind. Ergon.*, vol. 31, no. 3, pp. 149–160, Mar. 2003, doi: 10.1016/S0169-8141(02)00191-9.

[139] E. Welbergen, H. C. G. Kemper, J. J. Knibbe, H. M. Toussaint, and L. Clysen, "Efficiency and effectiveness of stoop and squat lifting at different frequencies," *http://dx.doi.org/10.1080/00140139108967340*, vol. 34, no. 5, pp. 613–624, 2007, doi: 10.1080/00140139108967340.

[140] K. B. Hagen, J. Hallen, and K. Harms-Ringdahl, "Physiological and subjective responses to maximal repetitive lifting employing stoop and squat technique,"

Eur. J. Appl. Physiol. Occup. Physiol. 1993 674, vol. 67, no. 4, pp. 291–297, Oct. 1993, doi: 10.1007/BF00357625.

[141] L. Straker and P. Duncan, "Psychophysical and psychological comparison of squat and stoop lifting by young females," *Aust. J. Physiother.*, vol. 46, no. 1, pp. 27–32, Jan. 2000, doi: 10.1016/S0004-9514(14)60311-1.

[142] J. H. Trafimow, O. D. Schipplein, G. J. Novak, and G. B. Andersson, "The effects of quadriceps fatigue on the technique of lifting.," *Spine (Phila. Pa. 1976).*, vol. 18, no. 3, pp. 364–367, Mar. 1993, doi: 10.1097/00007632-199303000-00011.

[143] A. Garg and G. D. Herrin, "Stoop or Squat: A Biomechanical and Metabolic Evaluation," *http://dx.doi.org/10.1080/05695557908974474*, vol. 11, no. 4, pp. 293–302, 2007, doi: 10.1080/05695557908974474.

[144] R. B. Graham, E. M. Sadler, and J. M. Stevenson, "Does the personal lift-assist device affect the local dynamic stability of the spine during lifting?," *J. Biomech.*, vol. 44, no. 3, pp. 461–466, Feb. 2011, doi: 10.1016/J.JBIOMECH.2010.09.034.

[145] S. J. Baltrusch, J. H. van Dieën, S. M. Bruijn, A. S. Koopman, C. A. M. van Bennekom, and H. Houdijk, "The effect of a passive trunk exoskeleton on metabolic costs during lifting and walking," *https://doi.org/10.1080/00140139.2019.1602288*, vol. 62, no. 7, pp. 903–916, Jul. 2019, doi: 10.1080/00140139.2019.1602288.

[146] M. M. Alemi, J. Geissinger, A. A. Simon, S. E. Chang, and A. T. Asbeck, "A passive exoskeleton reduces peak and mean EMG during symmetric and asymmetric lifting," *J. Electromyogr. Kinesiol.*, vol. 47, pp. 25–34, Aug. 2019, doi: 10.1016/J.JELEKIN.2019.05.003.

[147] A. S. Koopman *et al.*, "Biomechanical evaluation of a new passive back support exoskeleton," *J. Biomech.*, vol. 105, p. 109795, May 2020, doi: 10.1016/J.JBIOMECH.2020.109795.

[148] A. A. Simon, M. M. Alemi, and A. T. Asbeck, "Kinematic effects of a passive lift assistive exoskeleton," *J. Biomech.*, vol. 120, p. 110317, May 2021, doi: 10.1016/J.JBIOMECH.2021.110317.

[149] M. T. Picchiotti, E. B. Weston, G. G. Knapik, J. S. Dufour, and W. S. Marras, "Impact of two postural assist exoskeletons on biomechanical loading of the lumbar spine," *Appl. Ergon.*, vol. 75, pp. 1–7, Feb. 2019, doi: 10.1016/J.APERGO.2018.09.006.

[150] D. Janjic, "[Android-type obesity and gynecoid-type obesity]," *Praxis (Bern. 1994).*, vol. 85, no. 49, pp. 1578–1583, Dec. 1996.

[151] K.-B. Kim and Y.-A. Shin, "Males with Obesity and Overweight," 2020, doi: 10.7570/jomes20008.

[152] U. G. Kyle, Y. Schutz, Y. M. Dupertuis, and C. Pichard, "Body composition interpretation: Contributions of the fat-free mass index and the body fat mass index," *Nutrition*, vol. 19, no. 7–8, pp. 597–604, Jul. 2003, doi: 10.1016/S0899-

9007(03)00061-3.

[153] A. Osborne *et al.*, "Prevalence of musculoskeletal disorders among farmers: A systematic review," *Am. J. Ind. Med.*, vol. 55, no. 2, pp. 143–158, Feb. 2012, doi: 10.1002/AJIM.21033.

[154] M. Alizadeh, G. G. Knapik, P. Mageswaran, E. Mendel, E. Bourekas, and W. S. Marras, "Biomechanical musculoskeletal models of the cervical spine: A systematic literature review," *Clin. Biomech.*, vol. 71, pp. 115–124, Jan. 2020, doi: 10.1016/J.CLINBIOMECH.2019.10.027.

[155] A. Kiapour, A. Joukar, H. Elgafy, D. U. Erbulut, A. K. Agarwal, and V. K. Goel, "Biomechanics of the Sacroiliac Joint: Anatomy, Function, Biomechanics, Sexual Dimorphism, and Causes of Pain," *Int. J. Spine Surg.*, vol. 14, no. s1, pp. S3–S13, Feb. 2020, doi: 10.14444/6077.

[156] R. Izzo, G. Guarnieri, G. Guglielmi, and M. Muto, "Biomechanics of the spine. Part I: Spinal stability," *Eur. J. Radiol.*, vol. 82, no. 1, pp. 118–126, Jan. 2013, doi: 10.1016/J.EJRAD.2012.07.024.

국 문 초 록

육체적 부하가 큰 자세 및 동작으로 작업을 수행하는 것은 작업자의 근골격계 질환의 위험성을 증가시킨다. 작업자의 근골격계에 가해지는 육체적 부하의 양상은 수행하는 작업의 종류에 따라 달라진다. 장시간 앉은 자세로 작업을 수행하는 경우, 작업자의 근육, 인대와 같은 연조직에 과도한 부하가 발생하여 목, 허리 등 다양한 신체 부위에서 근골격계 질환의 위험성이 증가할 수 있다. 따라서, 착좌 시 발생할 수 있는 근골격계 질환의 위험성을 저감하기 위해서는 작업자의 착좌 자세를 실시간으로 모니터링하고, 이에 대한 피드백을 제공하는 것이 필요하다. 들기 작업과 같은 동적인 움직임이 포함된 작업을 수행하는 경우, 작업자의 체중이 신체적 부하에 영향을 미칠 수 있다. 전세계적인 비만의 유행으로 인해 많은 작업자들이 체중 증가를 겪고 있고, 들기 작업과 같은 동적인 작업에서 비만은 신체적 부하에 악영향을 미칠 수 있다. 따라서, 비만과 작업 관련 근골격계 질환의 위험성은 잠재적인 연관성을 가지고 있고, 비만이 들기 작업에 미치는 생체역학적 영향을 논의할 필요성이 있다.

작업장에서의 근골격계 질환의 위험성을 저감하기 위해 다양한 연구들이 수행되어 왔지만, 작업 시스템의 인간공학적 설계 측면에서 추가적인 연구가 필요하다. 장시간 의자에 앉아 정적인 작업을 수행하는 작업자의 근골격계 질환을 저감하기 위한 유망한 방법 중 하나로, 작업자의 자세를 실시간으로 모니터링하고

분류하는 시스템을 개발하는 것이 제안되고 있다. 이러한 시스템은 작업자가 근골격계 질환의 위험성이 낮은 자세를 작업 시간 동안 유지하도록 돕는 데 활용될 수 있을 것이다. 기존의 대부분의 자세 모니터링 시스템에서는 분류할 자세를 정의하는 과정에서 인간공학적 문헌이 거의 고려되지 않았고, 사용자가 실제로 활용하기에는 여러 한계점들이 존재하였다. 들기 작업의 경우, 체질량 지수(BMI) 40 이상의 초고도 비만 작업자의 동작 패턴을 논의한 연구는 거의 찾아볼 수 없었다. 또한, 다양한 들기 작업 조건 하에서 전신 관절들의 움직임을 생체역학적 측면에서 분석한 연구는 부족한 실정이다.

따라서, 본 연구에서의 연구 목적은 1) 다양한 센서 조합을 활용한 실시간 착좌 자세를 분류하는 시스템을 개발하고, 2) 들기 작업 시 초고도 비만이 개별 관절의 움직임과 들기 동작 패턴에 미치는 영향을 이해하여, 다양한 종류의 작업에서 발생할 수 있는 근골격계 질환의 위험성을 저감하는 것이다. 연구 목적을 달성하기 위해 다음의 두 가지 연구를 수행하였다.

첫번째 연구에서는 실시간으로 착좌 자세를 분류하는 스마트 의자 시스템을 개발하였다. 스마트 의자 시스템은 각각 여섯 개의 거리 센서와 압력 센서를 조합하여 구성되었다. 착좌 관련한 근골격계 질환에 대해 문헌 조사를 수행하였고, 이를 바탕으로 결정된 자세들에 대해 서른 여섯 명의 데이터를 수집하였다. 스마트 의자 시스템에서 자세를 분류하기 위해 kNN 알고리즘을 활용하였고, 성능을

검증하기 위해 단일 종류의 센서로 구성된 기준 모델들과 비교를 수행하였다. 분류 성능을 비교한 결과, 센서를 조합한 스마트 의자 시스템이 가장 우수한 결과를 보였다.

두번째 연구에서는 들기 작업을 수행할 때 초고도 비만이 개별 관절의 움직임과 동작 패턴에 미치는 영향을 분석하기 위해 모션 캡쳐 실험을 수행하였다. 들기 실험에는 근골격계 질환 이력이 없는 서른 다섯 명이 참여하였다. 수집된 데이터를 바탕으로 주요 관절(발목, 무릎, 엉덩이, 허리, 어깨, 팔꿈치) 별 운동역학적 변수들과, 들기 동작의 패턴을 표현하는 동작 지수들을 계산하였다. 들기 작업 조건과 비만 수준에 따라, 대부분의 변수에서 통계적으로 유의한 차이를 보였다. 전체적으로 비만인은 정상체중인에 비해 다리 보다 허리를 사용하여 들기 작업을 수행하였고, 동작 수행 시 상대적으로 적은 관절 각도 변화와 느린 움직임을 보였다. 들기 작업에서 박스의 이동에 개별 관절이 기여하는 비율도 정상체중인과 비만인은 다른 패턴을 보였다.

본 연구의 결과를 활용하여 다양한 종류의 신체적 부하에 노출된 작업자들의 근골격계 질환의 위험성을 저감할 수 있고, 궁극적으로 업무의 생산성과 개인의 건강을 제고할 수 있을 것이다. 첫번째 연구에서 개발된 스마트 의자 시스템은 기존 자세 분류 시스템의 단점들을 완화하였다. 개발된 시스템은 저렴한 소수의 센서만을 활용하여 근골격계 측면에서 중요한 자세들을 높은 정확도로 분류하였다. 이러한

자세 분류 시스템은 작업자에게 실시간으로 자세 피드백을 제공하여, 근골격계 질환의 위험성이 낮은 자세를 유지하는 데 활용될 수 있을 것이다. 두번째 연구의 결과는 동적인 작업 시 초고도 비만으로 인한 잠재적인 근골격계 질환의 위험성을 이해하는 데 활용될 수 있다. 초고도 비만인과 정상체중인 간 관절의 움직임과 동작의 차이를 이해하여, 비만을 고려한 인간공학적 작업장 설계와 동작 가이드라인을 제공할 수 있을 것이다.

주요어: 작업 관련 근골격계 질환, 육체적 부하, 자세 분류 시스템, 착좌 자세, 들기 작업, 비만, 관절 운동학, 동작 패턴

학번: 2015-21150